PETROGENESIS OF HIGH-GRADE METAMORPHIC SOLES FROM THE CENTRAL DINARIC OPHIOLITE BELT AND THEIR SIGNIFICANCE FOR THE NEOTETHYAN EVOLUTION IN THE DINARIDES

Branimir Šegvić*,✉, Damir Slovenec, Rainer Altherr***, Elvir Babajić°, Rafael Ferreiro Mählmann°°** and **Boško Lugović°°°†**

* *Department of Geosciences, Texas Tech University, Texas, U.S.A.*
** *Croatian Geological Survey, Croatia.*
*** *Institute for Geosciences, Ruprecht-Karls-Universität Heidelberg, Germany.*
° *Faculty of Mining, Geology and Civil Engineering, University of Tuzla, Bosnia and Herzegovina.*
°° *Institute of Applied Geosciences, Technische Universität Darmstadt, Germany*
°°° *Faculty of Mining, Geology and Petroleum Engineering, University of Zagreb, Croatia*
✉ *Corresponding author, email: branimir.segvic@ttu.edu*

Keywords: *high-grade metamorphic sole; supra-subduction zone; multi-stage metamorphism; Krivaja-Konjuh; Neotethys closure; Dinarides.*

ABSTRACT

High-grade metamorphic soles in NE Bosnia and Herzegovina make part of the Krivaja-Konjuh ophiolite complex (KKOC), which is one of the most important constituents of the Jurassic ophiolite mélange of the Central Dinarides. Several rock types were distinguished within the investigated metamorphic suite - sapphirine and corundum amphibolites, garnet-clinopyroxene±orthopyroxene amphibolites, clinopyroxene±garnet amphibolites, amphibolites per se and clinopyroxene+plagoclase±garnet gneisses. Peak temperature and pressure conditions calculated from different mineral pairs were estimated to range between 850 and 1100°C at 1.1 to 1.3 GPa. A prograde multi-stage metamorphic history of analyzed rocks was followed by the post-peak relaxation witnessed in decomposing porphyroblasts of garnet and ubiquitous formation of amphibole and orthopyroxene rims around clinopyroxene. The whole-rock chemical composition of magmatic protoliths largely defines it as cumulates from supra-subduction zones and scarcely as MORB-like tholeiitic mafic extrusives. Their origin is linked to near-ridge crust generation of a back-arc basin. Following the Middle Jurassic contraction of Neotethyan a portion of these rocks was likely entrained in an incipient subduction/thrusting system characteristic for the formation of metamorphic soles. According to geological evidences, and most notably, the age of radiolarians taken from KKOC basalts, the formation of metamorphic sole rocks must have followed a rapid transition in the Dinaridic Neotethys geotectonic setting before its final obduction onto the Adria margins in the next 15 Ma before the end of Jurassic.

INTRODUCTION

Metamorphic sole rocks accompany most of the Tethyan ophiolite complexes. They present high-grade metamorphic rocks that formed at temperatures of up to 1100°C, which structurally underlie the ophiolites (e.g. Pamić et al., 1973; Jamieson, 1986; Guilmette et al., 2008). The protoliths of these rocks are ocean-floor metabasites and, to a lesser extent, pelagic sedimentary rocks. Metamorphic conditions leading to the formation of the sole rocks are governed by high-temperatures and variable pressures existing below the hot sub-oceanic mantle of subduction zones (Gnos and Peters, 1993; Pamić et al., 2002). Geotectonic environments where metamorphic soles readily occur are the intraoceanic subduction zones in which metamorphism is linked to the onset of subduction regime (Lázaro et al., 2013). In other words, sole metamorphism usually denotes a change in ocean-floor dynamics (Dilek and Flower, 2003). This is the reason why metamorphic soles associated to ophiolites are studied worldwide, providing key information on ocean development and ophiolite emplacement history (e.g. Çelik and Delaloye, 2006; Guilmette et al., 2009; Šegvić et al., 2016).

This contribution investigates the high-grade metamorphic sole rocks associated to mantle ultramafites of the Krivaja-Konjuh ophiolite complex (KKOC), which is the biggest ophiolite complex in the Dinarides (Fig. 1). The Jurassic ophiolites of the Dinarides emerge as a narrow elongated zone that makes part of the Alpine-Himalayan-Tethyan orogenic belt (Robertson, 2002). Two belts of ophiolites are recognized in the Dinarides - the Central Dinaridic Ophiolite Belt (CDOB) in the west and the Vardar Zone in the east (Fig. 1). Both belts extend continuously to the south and are primarily composed of ophiolitic mélange consisting of magmatic blocks and various genetically-related sedimentary rocks (Dimitrijević and Dimitrijević, 1973). Recent palaeogeographic concepts advocate that Dinaridic ophiolites originate from the same marginal embayment of the Neotethys formed by westwards thrusting, which resulted in the current structural position of ophiolite units and related ophiolite mélange in the Dinaride-Hellenide nappe stack (Pamić et al., 1998; Gawlick et al., 2008; Schmid et al., 2008; Ustaszewski et al., 2010; Chiari et al., 2011; Bortolotti et al., 2013; Faul et al., 2014; Tremblay et al., 2015). An alternative approach favours the formation of spatially and geochemically distinct ophiolite domains from the two discrete oceanic branches of the Neotethys (Smith and Spray, 1984; Lugović et al., 1991; Robertson et al., 2013), which present a north-west continuation of the two oceanic domains recognized in the Hellenides (i.e. Pindos and Vardar basins, e.g. Ferrière et al., 2012).

The occurrences of metamorphic sole rocks in the Dinarides are not rare and, in addition to KKOC, major sole outcrops are documented throughout the mountain range (Pamić and Majer, 1973; Okrusch et al., 1978; Majer and Lugović,

Fig. 1 - Geotectonic schematic map of SE Europe showing Tethyan ophiolites stretching parallel to the Dinarides. The rectangle indicates a position of the Krivaja-Konjuh ophiolite complex (study area). Map modified after Robertson (2002).

1985; Robertson and Karamata, 1994; Srećković-Batoćanin et al., 2002; Milovanović et al., 2004; Palinkaš et al., 2008; Chiari et al., 2011). The age of metamorphism has been reported by several authors (Lanphere et al., 1975; Pamić et al., 2002; Karamata et al., 2005; Karamata, 2006) ranging between 181 to 146 Ma. This age correlates with the dating of radiolarian assemblages found in the chert-rich shaley to silty matrix of the Krivaja-Konjuh ophiolite mélange that was shown to be from Late Bajocian to Early Bathonian (Šegvić et al., 2014). Metamorphic soles in the Dinarides are usually lithologically diverse comprising of rocks from greenschist to granulite facies (Pamić et al., 2002; Milovanović et al., 2004; Šegvić, 2010). High-grade amphibolites and granulites are most abundant, and show a wide range of compositional and textural characteristics emerging predominantly as discontinuous thrust sheets below the blocks of peridotite (Roksandić, 1971; Chiari et al., 2011). Deformation features such as strikes of foliation overprint the sole and adjacent ultramafic rocks suggesting that both lithologies were folded together (Popević and Pamić, 1973). The peak metamorphic conditions for Vardar Zone high-grade soles were estimated to range from 0.50 to 1.20 GPa at temperatures greater than 800°C (Milovanović et al., 2004). In the CDOB, however, the P-T condition estimates rely on older literature (Pamić et al., 1973), which suggests that pressures range from 0.74 to 0.92 GPa at 650 to 750°C. Operta et al. (2003) provided P-T constraints for the KKOC corundum-bearing amphibolites fitting the range of 0.60 to 1.00 GPa at 620 to 830 °C. The whole-rock geochemistry of these rocks conforms with the nature of their oceanic igneous protoliths, which either points to cumulate gabbros or genetically related diabase-like rocks as plausible precursors (e.g. Pamić et al., 2002; Milovanović et al., 2004; Chiari et al., 2011). The mid-Jurassic metamorphic sole formation in the Dinarides marks a period of transition in the evolution of the Dinaridic Neotethys from ocean floor spreading to shrinking, ultimately leading to intraoceanic subduction and obduction processes. The onward obduction of the oceanic lithosphere ceased with the deposition of ophiolitic mélange on northern Adria margins in the footwall of the main mass of ultramafites and their associated metamorphic soles (e.g. Pamić et al., 2002; Chiari et al., 2011).

Despite the fact that the timing of ophiolite-related metamorphism in the Dinarides is relatively well known (Lanphere et al., 1975; Pamić et al., 2002; Karamata, 2006; Šegvić et al., 2014), no sufficient information exists to effectively constrain metamorphic conditions and petrogenetic processes that gave rise to the formation of metamorphic sole rocks in the Central Dinarides (especially in its western part, where modern analytical data are lacking or are not comprehensive). This research aims to contribute along those lines by presenting a thorough report on the overall mineralogical, petrological and geochemical characteristics of metamorphic rocks reported from the biggest ophiolite complex of the Dinarides (i.e. KKOC). Covering an area of 40 km^2, this large rock exposure is largely diverse with regards to its metamorphic parageneses (from granoblastic amphibolites to diopside gneisses), which provides an excellent petrological playground to study metamorphic sole genesis and plausible geodynamic scenarios responsible for its formation. Data on metamorphic sole from this part of the

CDOB, which is interpreted in conjunction with the related occurrences from the eastern parts of the Dinarides, Albanides and Hellenides, are essential for better comprehension of the late-stage dynamics of Dinaridic Neotethys during the period of Late Jurassic.

GEOLOGICAL SETTING

The ophiolite zone in the Dinarides presents a narrow and elongated portion of Alpine-type ultramafites and associated mafic and metamorphic sole rocks that extend from south of Zagreb, Croatia, and stretches further to the southeast through Bosnia and Herzegovina and west Serbia continuing south-west-wards to the Mirdita ophiolites in Albania (Fig. 1; e.g. Pamić et al., 1998; Karamata, 2006). Numerous occurrences of ophiolitic rocks are documented in the Dinarides, from relatively smaller rock blocks (m to km-size) usually being entirely altered to large sheets (massifs) covering as much as 1000 km^2 (e.g. Trubelja et al., 1995). The ophiolites are embedded in a mélange (Fig. 2; e.g. Dimitrijević and Dimitrijević, 1973; Šegvić et al., 2014). This mélange originated by tectonic deformation and at least partly by olistostrome mechanism and it consists of a sheared pelitic to silty matrix wherein besides the igneous rocks of various provenances the blocks of different sedimentary rocks are encountered (Pamić et al., 2002). The larger ophiolite complex, such as Krivaja-Konjuh, presents thrust sheets with the mélange being found in the footwall (Fig. 3; Tari, 2002). The emplacement of ophiolites in the Dinarides is linked to the initial oceanic crust décollement and subsequent obduction of the Late Jurassic crust along the continental passive margins of Adria (e.g. Pamić et al., 1977; Chiari et al., 2011). In terms of mineralogical composition, larger blocks and/or sheets often preserve undisturbed and, occasionally, complete ophiolite sequences (Pamić and Desmons, 1989), whereas smaller ophiolite blocks normally consist of one rock type only (Pamić et al., 2002). The metamorphic sole rocks usually occur as narrow zones (100 to 1000 m wide) around the main ultramafic blocks and/or sheets (Pamić et al., 1973).

The Krivaja-Konjuh ophiolite complex in NE Bosnia-Herzegovina (Fig. 1) has a surface of about 650 km^2 and shows a distinct NW-SE elongation, with the longer axis being around 40 km and the shorter of maximally 20 km in size (Fig. 2; Pamić et al., 1977; Pamić and Hrvatović, 2000).

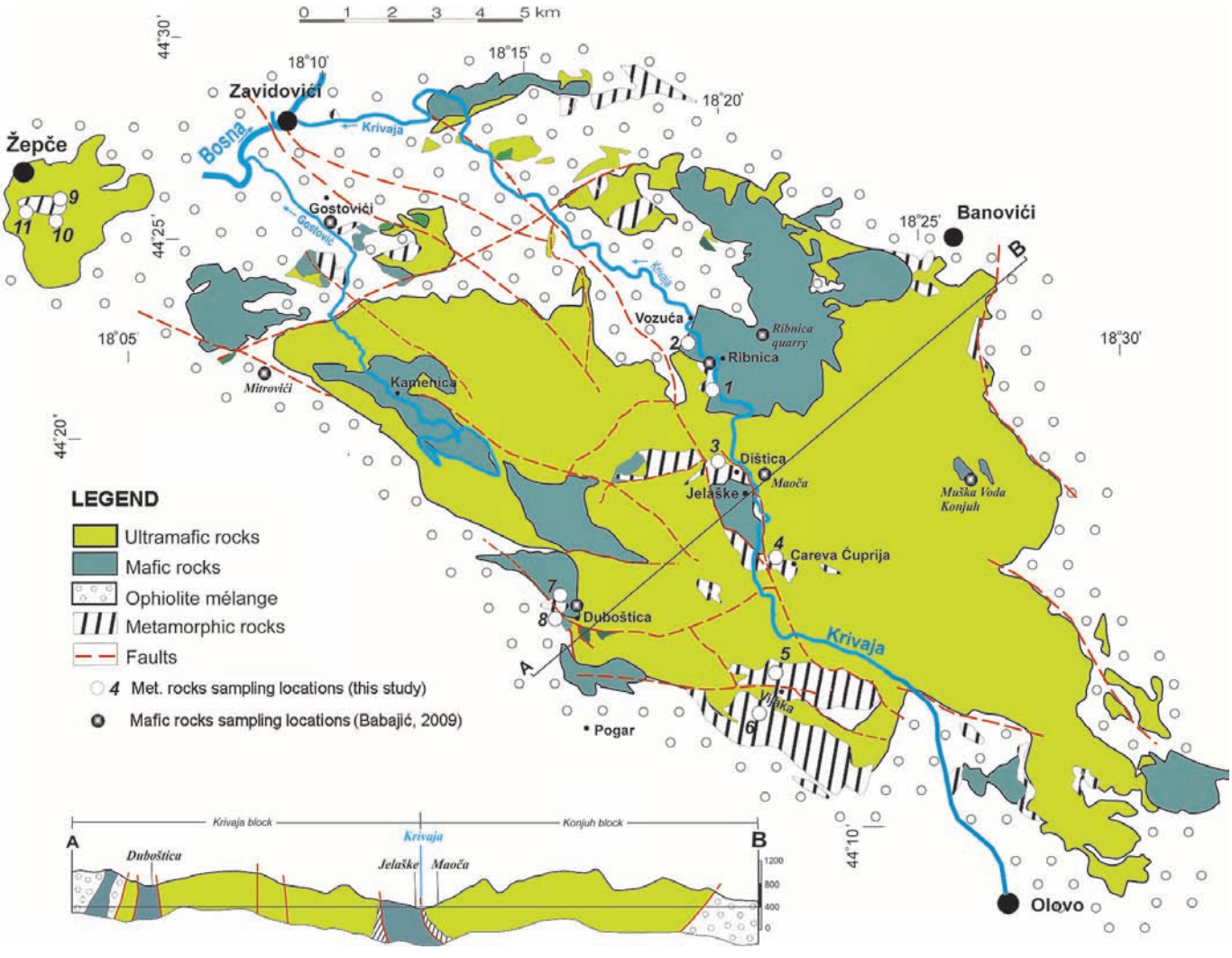

Fig. 2 - Simplified geological map of the Krivaja-Konjuh ophiolite complex. Modified after Pamić (1968; 1970), and Đorđević and Pamić (1972). Sampling locations of metamorphic sole rocks (1-11) are provided with details available in Table 1. Sampling locations of mafic rocks are from Babajić (2009) with reference to Table 5. The SW-NE cross-section A-B depicts a tectonic nature of the contact between large blocks of ultramafites and subordinate mafic rocks.

According to seismic profiles, the complex renders a basal and slightly concave sheet with an estimated maximal thickness of 2 km (Roksandić, 1971). The sheet is separated in (at least) two large blocks, Krivaja, the western block made of amalgamated ultramafites and associated mafic rocks, Konjuh, the eastern and relatively coherent block predominantly represented by peridotites (Fig. 2; Pamić, 1970; Đorđević and Pamić, 1972). Integral part of this complex makes a smaller, a few kilometres large bloc, and Žepče, placed at the most NW of the complex. It consists of ultramafic rocks and some minor metamorphic sole rocks (Fig. 2). Being detached as solid parts of the oceanic crust and later tectonically incorporated in the mélange matrix these ophiolite blocks are locally thrust onto the lower portion of mélange matrix (Fig. 3). A complete Krivaja-Konjuh ophiolite sequence is thrust on Early and Middle Jurassic non-ophiolitic sedimentary sequences, and is overlaid by the Cretaceous basinal Pogari formation (Fig. 3; Pamić, 1970; Hrvatović, 2006). The mélange of the Krivaja-Konjuh ophiolite complex presents a chaotic lithological unit in which primary depositional sequences are rarely preserved due to subsequent tectonic activity. It is furthermore characterized by pelitic to silty matrix featured by decimetre to several hundred meters size blocks of oceanic crust merged with Palaeozoic to Jurassic carbonate and clastic sedimentary rocks (Fig. 2; Tari, 2002). The occurrence of barely preserved Jurassic foraminifera (*Vidalina martana, Glomospira sp., Cristellariasp.*, Pamić and Hrvatović, 2000) documented from micrites interlayered with shales and greywackes is consistent with the Latest Bajocian to Early Bathonian radiolarian assemblage obtained from chert-rich shaly to silty matrix, which effectively defines the Late Jurassic age of ophiolite mélange (Fig. 3; Šegvić et al., 2014). The Krivaja-Konjuh ophiolite complex is largely made of lherzolite (~ 80%; Pamić, 1968; Pamić, 1970; Đorđević and Pamić, 1972) with some minor occurrences of dunite and pyroxenite (Pamić et al., 1977; Maksimović and Majer, 1981; Maksimović and Kolomejceva-Jovanović, 1987; Lugović et al., 1991; Trubelja et al., 1995; Šegvić, 2010). Gabbro is the main mafic rock type often featured by distinctive cumulitic textures and is usually reported as being associated with the large ultramafic blocks (Pamić et al., 1977; Babajić, 2009; Šuica et al., 2018). The contact of the main peridotite block with mélange rocks is solely tectonic with an enhanced serpentinization of peridotites reported along the contact zones (Pamić et al., 1977).

The eastern ultramafic block - Konjuh - conformably overlies a zone that is up to a 10 km long and several hundred meters wide consisting of metamorphic sole rocks, which are composed of greenschist to granulite facies rocks (Fig. 2; Pamić et al., 1977; Operta et al., 2003; Šegvić, 2010). Minor amounts of metamorphic sole rocks are also observed further to the northwest in an area that follows the

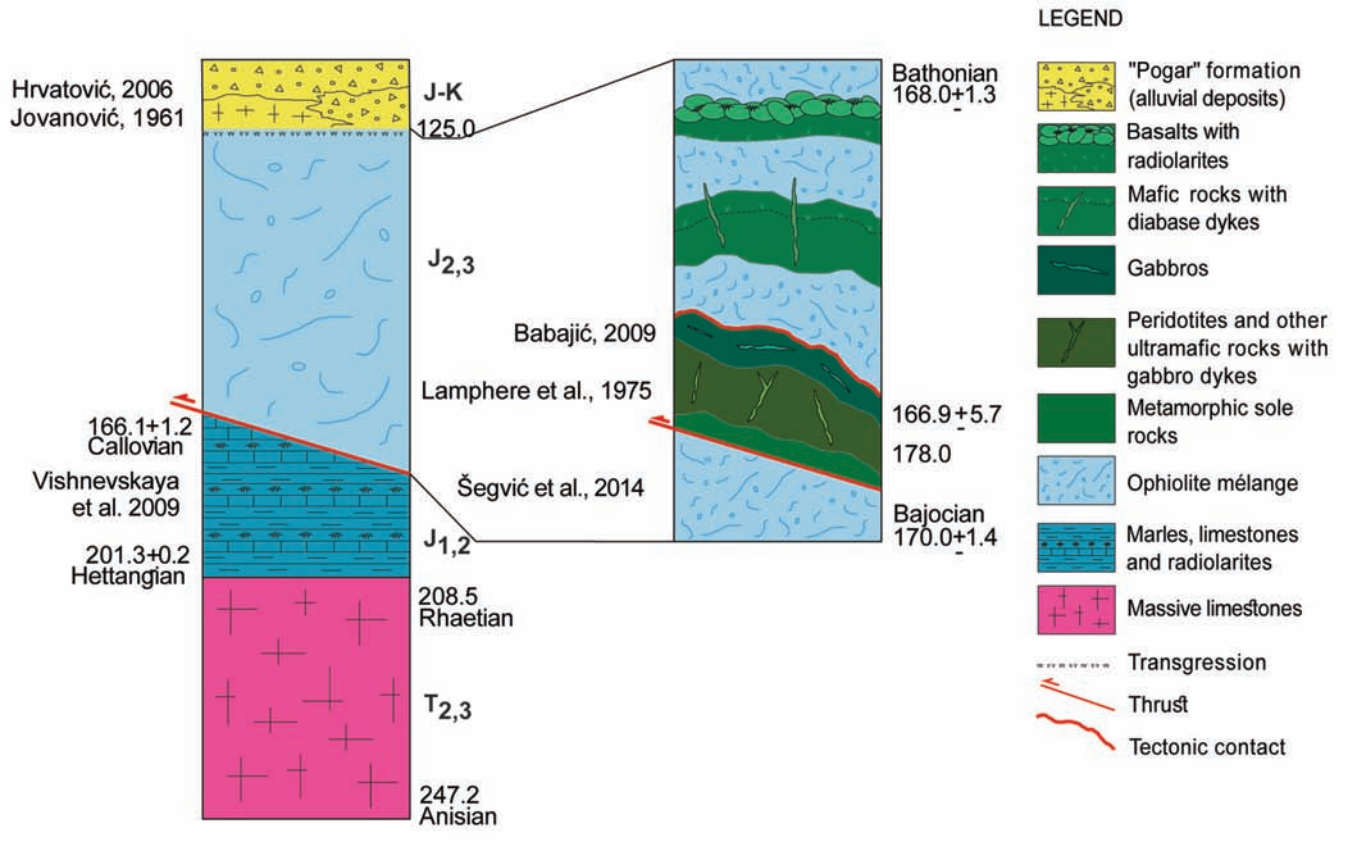

Fig. 3 - Composite stratigraphic section of the KKOC with a zoomed section that depicts the composition of the ophiolite mélange. Constructed after basic geological map of Yugoslavia (Pamić, 1968; 1970; Đorđević and Pamić, 1972). Time scale after Gradstein and Ogg (2012). Late Triassic age based on palaeontological evidences (Pamić, 1968). Early and Middle Jurassic age described from non-ophiolitic sedimentary sequences (Vishnevskaya et al., 2009). Middle Jurassic age documented from the radiolarian assemblages found in the chert-rich shaley to silty matrix of the ophiolite mélange (Šegvić et al., 2014). Early and Middle Jurassic age of amphibolites and gabbros based on radiometric dating (Lanphere et al., 1975 and Babajić, 2009, respectively). Cretaceous age of the "Pogari" series inferred on palaeontological evidences (*Tintinopselcarpathica, Tintinopsellaoblonga, Lithostrobus sp., Calponellopsis sp.,* Jovanović, 1961; Hrvatović, 2006).

main fault that separates two ultramafite blocks (Fig. 2; Šegvić, 2010). Metamorphic sole rocks are suggested to represent the deepest portion of the Jurassic ophiolite sequence, which is thrust onto the basal section of ophiolitic mélange matrix (Fig. 3). The contact with the mélange was not documented neither in this study nor in any of earlier works in the area (Pamić et al., 2002 and references therein). On the other hand, the joining of metamorphic sole rocks and the overlying ophiolite member consisting of peridotites, gabbro-peridotites and gabbros (Fig. 3) is either primary (Fig. 4a-b) or more rarely tectonic (Fig. 4c-d). The metamorphic sole rocks in the area of Vijaka and Duboštica (Fig. 2) show a clear lithological zonation with granulite facies rocks that are exposed proximally to the contact with peridotites, while the rocks belonging to amphibolite and epidote-amphibolite facies normally occur relatively farther from the contact (Pamić et al., 1977; Šegvić, 2010).

Compositions of a range of mafic rocks cropping out within the Krivaja-Konjuh ophiolite complex (analyses taken from Babajić, 2009) were examined in a search for plausible protoliths of the investigated metamorphic sole. Compared to ultramafites, mafic rocks are less frequent, making about 10% of the entire massif (Pamić et al., 1977). They are principally encountered in the centre of the massif (Pamić et al., 1977) and along its eastern and northern margins (Trubelja, 1961; Ristić and Likar, 1967). According to Babajić (2009), mafic rocks of Krivaja-Konjuh consist of massive intrusives (isotropic gabbroides and some minor troctolites), extrusives (basalts, spilites, dolerites), and sporadic dykes composed of microgabbros and gabbronorites. Isotropic gabbroic rocks (gabbros, gabbronorites, amphibole gabbronorites, and anorthosites) constitute the most abundant mafic variety in the Krivaja-Konjuh ophiolite complex largely cropping out at Duboštica and Ribnica (Fig. 2). Rocks are partly characterized by secondary mineral assemblages made of albite, prehnite, and tremolite-actinolite, which is compatible with very-low grade to low grade metamorphic overprint. Troctolites of Gostovići and Maoče (Fig. 2) represent the cumulate mafic to ultramafic rocks. Olivine and plagioclase emerge as cumulate phases, while intercumulus liquids gave rise to the crystallization of minor clinopyroxene. Extrusive rocks have a massive texture (basalts and dolerites of Ribnica and Duboštica, Fig. 2) and only rarely are they reported in form of pillow lavas characteristic for submarine volcanism (spilites of Ribnica and Mitrovići, Fig. 2). Solely dolerites stand for relatively fresh extrusive rocks with the typical ophitic to intergranular texture. Dykes of extrusive rocks (diabases/microgabbros) are reported in the

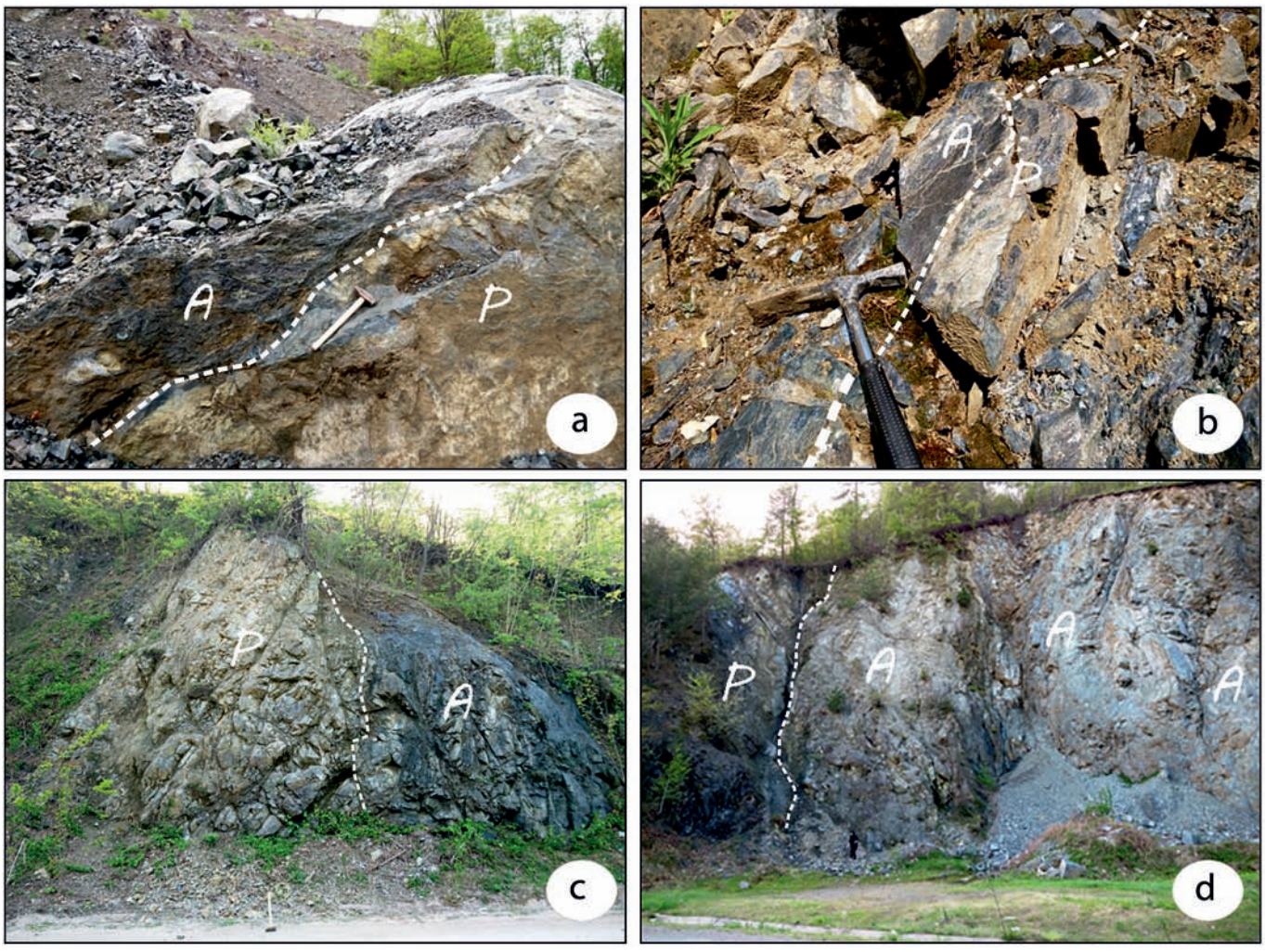

Fig. 4 - (a) and (b) Field photographs showing a primary contact between metamorphic sole rocks (A) and serpentinized peridotites (P) in the vicinity of Žepče (Fig. 2), (c) and (d) Photographs showing a tectonic contact between metamorphic sole rocks (A) and serpentinized peridotites (P) in the area of Ribnica (Fig. 2).

host basalts and spilites (Ribnica, Fig. 2). They are fresh and commonly show quench textures at the contact with the surrounding rocks. Dykes of intrusive rocks (gabbronorites) are typically reported cutting the foliated lherzolites that are characterized by clusters of pyroxene set in a medium to small grained olivine matrix ("berry-like" lherzolite, Šegvić, 2010). Gabbronorite dykes are dominated by plagioclase, which is in turn responsible for their leucocratic appearance.

MATERIALS AND METHODS

The rocks were sampled from 11 localities (Table 1) scattered within the large amphibolite mass at the south of the complex (Fig. 2; Vijaka and Duboštica localities) and in the smaller outcrops placed along the major fault zone that separates the two main ultramafite blocks (Fig. 2; Krivaja, Krivaja-Vozuća, Maoča, and Careva Ćuprija localities). In the latter case the rocks were gathered either from fresh outcrops (Maoča, Careva Ćuprija) or, in the event of outcrop unavailability, from the coarse sediment (boulders) recovered from mountain streams rich in high-grade metamorphic pebbles (Krivaja and Krivaja-Vozuća). Additional sampling localities encompassed a metamorphic terrain in the vicinity of the town of Žepče (Fig. 2), which represent a tectonically displaced part of the Krivaja-Konjuh ophiolite complex that crops out along the creeks of Ograjna (Pamić et al., 1977 and references therein) and Papratnica (Šegvić et al., 2014). From a total of 67 thin-sections, 19 representative samples were analyzed by microbeam techniques (SEM-EDS and EPMA) and geochemical whole-rock analyses (XRF and ICP-MS). An overview on the sample selection with the corresponding rock types and field information is provided in Table 1, while Table 2 offers more details on metamorphic rock types and their critical mineral parageneses.

The chemical composition of minerals was measured by electron probe microanalyzer (EPMA) at the Institute of Geosciences (University of Heidelberg/Germany) using a CAMECA SX51 equipped with a five wave length-dispersive spectrometers. Operating parameters include 15 kV accelerating voltage, 20 nA beam current, ~ 1 μm beam size, and 10 seconds counting time for all elements. Natural minerals, oxides (corundum, spinel, hematite, and rutile), and silicates (albite, orthoclase, anorthite, and wollastonite) were used for calibration. The measurements relative error was less than 1%. Raw data were corrected for matrix effects using the PAP algorithm (Pouchou and Pichoir, 1984; Pouchou and Pichoir, 1985) implemented by CAMECA. Mineral phase formula calculations were done using a software package designed by H-P. Meyer (University of Heidelberg/Germany). The rock textures and morphology of the main mineral phases in the same set of samples have been investigated by scanning-electron microscope equipped with an EDS system (SEM-EDS). The instrument used is Leo 440 REM with an integrated Oxford Inca EDS installed at the Institute of Geosciences (University of Heidelberg/Germany). A variety of acceleration voltages and beam size conditions were employed to assure the best imaging conditions.

Whole-rock chemical analyses were done by the X-ray fluorescence (XRF) and inductively coupled plasma-mass

Table 1 - List of sampling localities and types of metamorphic rocks investigated.

Locality	Samples	Fig. 2	GPS	Types of metamorphic rocks (Table 2)	Rock texture	Rock structure
Krivaja	MK2	1	4910405, 6520980	metagabbro (MC)	porphyroblastic	banded and foliated
Krivaja –Vozuća	U29, U30	2	6530130, 4914136	meta-troctolites (MC)	granoblastic	banded and foliated
Maoča	GR7, R8	3	4905700, 6534230	metagabbros (MC)	porphyroblastic (GR7) / granoblastic (R8)	massive
Careva Ćuprija	CC1	4	4900280, 6530540	metagabbro (MC)	porphyroblastic	massive
Vijaka Stream	V1, U40	5	4890840, 6530510	metagabbros (MC)	porphyroblastic	banded and foliated
Vijaka South	V4, X1	6	4890685, 6530440	metagabbros (MC)	granoblastic (V4) / porphyroblastic (X1)	banded and foliated
Duboštica North	U22	7	4900270, 6520595	metagabbro (MC)	porphyroblastic	banded and foliated
Duboštica	DU5, U23	8	4900060, 6520510	metabasalt, metagabbro (MC)	porphyroblastic (DU5) / granoblastic (U23)	banded and foliated
Žepče - Papratnica	Z1C	9	4920689, 6498823	metabasalt	gneissic	banded
Žepče – Ograjna 1	10D	10	4919447, 6498759	metabasalt	gneissic	banded
Žepče – Ograjna 2	11C	11	4920021, 6497938	metabasalt	granoblastic	massive

MC- meta-cumulate.

Table 2 - Classification and mineral parageneses of the Krivaja-Konjuh metamorphic soles.

META-CUMULATES (MC)		METABASALTS (MB)
Meta-troctolites	**Metagabbros**	
Spr-bearing amphibolite	*Grt + Cpx ± Opx-bearing amphibolite*	*Cpx ± Grt amphibolite*
Sample U30	*Samples CC1, U22, MK2, GR7, V1, X1, U40, V4*	*Samples 11C, DU5*
Crn-bearing amphibolite	*Amphibolite*	*Cpx + Pl ± Grt gneiss*
Sample U29	*Samples R8, U23*	*Samples 10D, Z1C*

SAMPLE	ROCK TYPE	MAIN PHASES	MINOR PHASES
U30	Spr-bearing amphibolite (MC)	Amp, Pl, Czo	Spr, Sp
U29	Crn-bearing amphibolite (MC)	Amp, Pl, Crn,	Czo, Ct, Pmp, Cc, Cpx, Sp
CC1	Grt + Cpx ± Opx-bearing amphibolite (MC)	Grt, Amp, Pl, Cpx, Rt	Ttn, Cc, Ilm
MK2	Grt + Cpx ± Opx-bearing amphibolite (MC)	Grt, Amp, Pl, Cpx, Opx	Mt
GR7	Grt + Cpx ± Opx-bearing amphibolite (MC)	Grt, Amp, Pl, Cpx, Opx	Mt
V1	Grt + Cpx ± Opx-bearing amphibolite (MC)	Grt, Amp, Pl, Cpx, Opx	Mt
U22	Grt + Cpx ± Opx-bearing amphibolite (MC)	Grt, Amp, Pl, Cpx	Chl
X1	Grt + Cpx ± Opx-bearing amphibolite (MC)	Grt, Cpx, Pl, Amp, Opx	Rt, Mt
U40	Grt + Cpx ± Opx-bearing amphibolite (MC)	Grt, Cpx, Pl, Amp, Opx	Rt, Mt
V4	Grt + Cpx ± Opx-bearing amphibolite (MC)	Grt, Cpx, Pl, Amp, Opx	Mt
R8	Amphibolite (MC)	Amp, Pl, Ttn, Prh	Ilm, Ap, Chl
U23	Amphibolite (MC)	Amp, Pl, Ttn, Prh	Ilm, Ap, Chl
11C	Cpx ± Grt amphibolite (MB)	Amp, Pl, Czo, Prh, Ilm, Cpx	Ttn, Ap, Pmp, Chl
DU5	Cpx ± Grt amphibolite (MB)	Grt, Amp, Pl, Cpx, Ttn	Xo
10D	Cpx + Pl ± Grt gneiss (MB)	Amp, Cpx, Pl	Ttn, Ilm, Ap, Prh
Z1C	Cpx + Pl ± Grt gneiss (MB)	Grt, Cpx, Pl, Sp, Opx, Ilm	Ttn

spectrometry (ICP-MS) on a set of 19 selected samples. Conventional energy dispersive XRF, using the Siemens SRS 303 instrument, was performed at the Institute of Geosciences (University of Heidelberg/Germany), whereas the ICP-MS measurements were done at the Bureau Veritas (ACME) laboratory in Vancouver, Canada. The XRF measurements were carried out on glass beads obtained by $Li_2B_4O_7$ powder fusion in a platinum crucible at 1150°C. For microelements, beads produced by pastel ceramic-powder pressing, were used. Repeated analyses of different sample aliquots indicated a relative standard deviation of ±5%. The accuracy of the analyses with respect to the USGS international reference standard DNC-1/A for macro elements fits the range of ±8%. The ICP-MS measurements were performed on 0.2 g of sample, which followed a lithium metaborate/tetraborate fusion and diluted nitric digestion. Loss on ignition (LOI) was acquired by weight difference, after ignition at 1000 °C. The quality of the analyses was monitored by comparison to standard samples provided by ACME.

Geothermobarometric calculations are based on the compositions of thermodynamically equilibrated pairs of different mineral phases. Metamorphic temperatures were estimated using the geothermometers of Spear (1980) and Holland and Blundy (1994) (*amphibole-plagioclase*), Krogh (1988) (*garnet-clinopyroxene*), Harley (1984) and Lee and Ganguly (1988) (*garnet-orthopyroxene*), Graham and Powell (1984) and Krogh Ravna (2000) (*garnet-amphibole*), and Wells (1977) and Brey and Köhler (1990) (*two pyroxenes*). For the estimation of metamorphic pressures, the following geobarometers were employed: Schmidt (1992) (*Al in amphibole*), Newton and Perkins (1982) (*garnet-clinopyroxene-plagioclase*), Harley and Green (1982) and Nickel and Green (1985) (*garnet-orthopyroxene*), Paria et al., (1988) (*orthopyroxene-clinopyroxene-garnet-plagioclase*), and Perkins and Chipera (1985) (*orthopyroxene-garnet-plagioclase*). Peak metamorphic P-T conditions have been additionally defined through the related reaction curves, calibrated for the basaltic system (NCFMASH and CFMASH). Peak-metamorphic P-T conditions of granulite facies rocks can often be reset by diffusion, which is referred in the literature as 'granulite uncertainty principle', mostly taking place in the slow cooling terrains (Harley, 1989). However, analyzed rocks are believed to have been formed by the rapid metamorphic event that experienced fast cooling during ophiolite obduction thus preserving the peak-metamorphism mineral assemblages. The mechanism explaining such a metamorphic overprint and subsequent rapid cooling is usually linked to the inverted metamorphic gradient fields exhibited by many soles (Spray, 1984). Namely, the inverted temperature anomaly responsible for the high-grade metamorphism of the sole parishes quickly (< 2 Ma) as subduction continues (Peacock, 1988; Hacker, 1990; 1991; Harper et al., 1996). It follows that the high-grade metamorphism of the sole occurs only at the inception of the subduction because the hanging wall would be too cold to maintain high-grade metamorphism thereafter (Wakabayashi and Dilek 2003; Wakabayashi, 2004).

Mineral abbreviations after Kretz (1983). Amp- amphibole; Pl- plagioclase; Czo- clinozoisite; Spr- sapphirine; Sp- spinel; Crn- corundum; Ct- clintonite; Pmp- pumpellyite; Cc- calcite; Ilm- ilmenite; Grt- garnet; Cpx- clinopyroxene; Opx- orthopyroxene; Mt- magnetite; Chl- chlorite; Rt- rutile; Ttn- titanite; Illm- ilmenite; Ap- apatite; Prh- prehnite; Ep- epidote; Xo- xonotlite; Modal mineralogy of minor phases were reported not to exceed 5 vol% following the thin-section visual inspections.

RESULTS

Rock fabric

The main amphibolite mass of the Krivaja-Konjuh ophiolite complex is placed along its southern margins and represents the deepest member of the ophiolite sequence identified in the composite ophiolite mélange of the Dinarides (Fig. 2; Vijaka and Duboštica). Smaller metamorphic outcrops can also be traced along the junction of the two main ophiolite blocks (Fig. 2; Krivaja, Maoče and Careva Ćuprija). Recovered rocks' textures are largely crystalloblastic (i.e. granoblastic to nematoblastic) and are defined by the elongation of amphibole (Fig. 5a-c; Table 1). Analogue texture in garnet-bearing rocks is defined as porphyroblastic (Fig. 5b-d; Table 1). In case of the rocks defined by the conspicuous alternation of mineral domains the texture was defined as gneissic (Table 1). The structure of the rocks is either massive or banded to foliated. The former is rare and is characteristic for the central zone of the KKOC (Fig. 5a-b; Maoče and Careva Ćuprija). Banded structures with marked lineations are commonly observed in the Dubošti-ca-Vijaka-Krivaja amphibolite. The alternation of 'bright' and 'dark' rock portions define such banded structural varieties (Fig. 5c-d). Bright portions are predominantly composed of plagioclase, whereas dark ones are foliated to lineated and consist of black to pale-green amphibole. Mineral grain sizes vary considerably depending on the sample with an average range from 0.3 to 1.0 mm. Based on the rock fabric, the sole rocks from the Krivaja-Konjuh ophiolite complex were divided into five groups: (a) homogenous massive (granular to nematoblastic) metamorphites (Fig. 5a, Table 1, Maoče), (b) homogenous porphyroblastic metamorphites (Fig. 5b, Table 1, Careva Ćuprija), (c) banded massive metamorphites (Fig. 5c, Vijaka), (d) banded porphyroblastic metamorphites (Fig. 5d, Table 1, Duboštica) and (e) banded gneissic metamorphites (Table 1, Žepče).

Petrography and mineral chemistry

The prevailing metamorphic textures of the KKOC soles were shown to be either granoblastic or porphyroblastic. The former are defined by the coarse blasts of amphibole and plagioclase, while the latter are dominated by the blasts of garnet (0.2–10 mm in size) merged in a fine-grained homogenous matrix (Fig. 5). A clear geochemical discrimination exhibited by analyzed rocks (i.e. meta-cumulates vs. metabasalts) has been taken as a base for their further classification (Table 2). The meta-cumulates may thus be divided into meta-troctolite and metagabbro. The former is consisted of Spr-bearing and Crn-bearing amphibolite, while the letter count for Grt-Cpx (±Opx) amphibolite and amphibolite per se. Metabasalts are either Cpx±Grt amphibolite or Cpx-Pl±Grt gneiss.

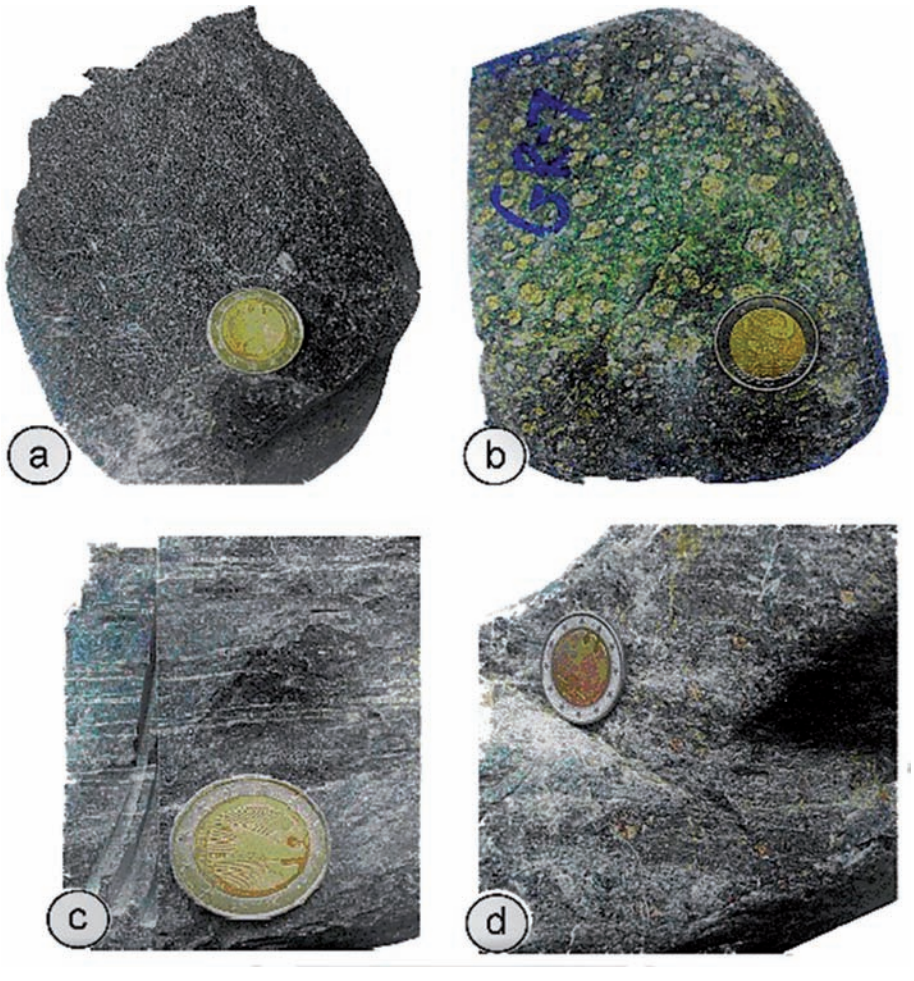

Fig. 5 - Photographs showing a variety of the KKOC metamorphic sole rocks (a) homogenous massive (granular to nematoblastic) metamorphites; (b) homogenous porphyroblastic metamorphites; (c) banded massive metamorphites, and (d) banded porphyroblastic metamorphites. For details see the text.

Spr-bearing amphibolite (meta-troctolite 1)

is made of amphibole, plagioclase, clinozoisite, sapphirine and Cr spinel (Tables 1 and 2). Rock is dominated by the medium to coarse grained amphibole (Fig. 6a) whose composition corresponds to tschermakitic hornblende (Fig. 7a). The interstitial space defined by amphibole blasts is filled by An-rich plagioclase that tapers at the tips. Secondary clinozoisite (Table 3) is relatively abundant formed at the expense of anorthite (Fig. 6b). The coarse grains of relict Cr-spinel (0.2-0.5 mm) are commonly included in the blue pleochroitic blasts (~ 0.5 mm) of Al-rich sapphirine (Fig. 6c; Table 3) where they seem to be intrinsically unstable. In this rock type tschermakitic hornblende and anorthite appear to be texturally equilibrated showing simple grain boundaries and triple-point contacts. Conversely, the sapphirine crystals are found in textural disequilibrium with the surroundings which is manifested by extensive grain boundary migrations (Fig. 6d). Sapphirine formation in silica unsaturated metamorphic systems requires a peraluminous environment and higher degrees of metamorphism (Gnos and Kurz, 1994). The growth of sapphirine at the expense of relict spinel may, therefore, reflect the oscillating peak metamorphic conditions that were coupled with a progressive silification which effectively put an end to sapphirine growth (e.g. Deer et al., 1996).

Crn-bearing amphibolite (meta-troctolite 2)

mineral paragenesis is consisted of amphibole, plagioclase, corundum and minor phases such as clinopyroxene, clinozoisite, Al and Cr spinel, clintonite, Al-pumpellyite, and calcite (Tables 1 and 2). The Crn-bearing amphibolite was reported solely at the Krivaja locality but Operta et al. (2003) reported on its presence at the south of the Krivaja-Konjuh ophiolite complex (the Vijaka locality). Grains of medium-sized amphibole and corundum (~ 0.15 mm) define the rocks' granoblastic texture. The amphibole interstitial space is largely filled by the relics of euhedral calcic plagioclase. Amphibole's chemistry is exclusively pargasitic (Table 3; Fig. 7b) with no record of retrograde varieties. Plagioclase is rich in calcic component (99.9% An; Table 3; Fig. 7c) and it tends to alter rapidly into the secondary albite and clinozoisite. The subhedral blasts of corundum are mainly rod-shaped and are regularly found rimmed by Mg-Al spinel (Fig. 6e). The composition of corundum is very uniform (Al_2O_3 content ~ 99 to 100 wt%). Spinel is an Al-rich variety with a composition of pleonaste (Table 3). Several authors explain the formation of spinel coronas through the reaction of corundum and Mg-rich calcite yielding spinel and carbon-dioxide (e.g. Nitch et al., 1985; Liati, 1988). In this rock type an Al-rich mica is occasionally preserved as a corundum's tiny second rim (Fig. 6f). Its chemistry ($Ca_{0.928\text{-}0.993}Mg_{1.923\text{-}2.016}Al_{5.416\text{-}5.686}Si_{2.203\text{-}2.469}O_{10}(OH)_2$) closely corresponds to the one of clintonite. A post-peak event coupled with higher water activity in a peraluminous environment must have caused the formation of Al-rich retrograde phases (i.e. pleonaste and clintonite). Small relicts of presumably igneous clinopyroxene (Al_2O_3 content of 6.5-11.3 wt%) are present in this rock type (Fig. 6f). They do not exhibit preserved crystal shapes due to the strong amphibole overgrowth. No mutual contact between clinopyroxene and other minerals but amphibole were documented which suggests a lack of textural equilibrium of clinopyroxene with other metamorphic phases (e.g. Moazzen and Oberhänsli, 2008). In favour of such a reasoning is the clinopyroxene phase chemistry (Table 3; Fig. 8b) which is, compared to the bulk of analyzed clinopyroxene, Fe impoverished and richer in Ca. Apart of clinopyroxene, Cr-rich spinel is yet another relict phase frequently encountered in pargasite granoblasts (Table 3).

Grt-Cpx±Opx amphibolite (metagabbro 1)

is the most common metamorphic rock type within the Krivaja-Konjuh ophiolite complex (Tables 1 and 2). This rock type may be further divided into the subgroup where orthopyroxene has not been reported (samples CC1 and U22) and subgroup where orthopyroxene is either a product of garnet dissolution (samples MK2, GR7 and V1) or it is found texturally equilibrated with the neighbouring phases (samples X1, U40 and V4). Mineral paragenesis of the first subgroup is consisted of garnet, amphibole, clinopyroxene, and plagioclase while rutile, titanite, ilmenite, magnetite and orthopyroxene are minor phases (Table 2). The texture is typically porphyroblastic delineated by a medium to coarse-grained blasts of garnet (up to 1 cm in size) that come along with the sub-rounded clinopyroxene and amphibole (up to 1 mm in size; Fig. 6g). The matrix is homogenous and made of amphibole, clinopyroxene, plagioclase and minor phases. Garnet crystalloblasts largely fit into the pyrope-almandine compositional span (Table 3; Fig. 8a) and barely shows any compositional zoning. There is only a smaller number of blasts featured by a weak "U"-shape compositional trend defined by the pyrope's component, whilst the almandine component produced an opposite trend. Such homogeneity in garnet chemistry suggests phase equilibration at peak metamorphic conditions (e.g. Woodsworth, 1977) whereas the feeble Py-Alm zonation renders a sign of prograde metamorphism (e.g. Romano et al., 2006). Garnet commonly embeds the inclusions of clinopyroxene, amphibole, plagioclase, rutile and titanite. Occasionally the porphyroblasts of garnet (sample MK2) are featured by a system of rutile needles with an apparent crystallographic orientation ({111} direction of garnet) (Fig. 6h). Such a microparting in garnet is thought to be a strain response to the pressure at the time of peak metamorphism (Hwang et al., 2007). Micro-scale partial melts, characteristic for high-grade peak metamorphism, might have had reacted with garnet, hence precipitating the oriented rutile needles. Kelyphitic coronas are commonly developed around garnet porphyroblasts having an average width of 30 μm (Fig. 6i). They contain plagioclase, orthopyroxene, and magnetite (Fig. 6j) which is a result of garnet's retrograde recrystallization. Garnet from such coronas has analogue chemistry to the one of fresh porphyroblasts. On the other hand, plagioclase is fairly calcic (~ 90% An) which is typical for the low-temperature plagioclase formation at the expense of unstable garnet (Baldwin et al., 2003). Kelyphitic orthopyroxene usually has a pinkish own colour forming radial intergrowths with magnetite. Its chemistry corresponds to hypersthene (Table 3). The highest Al_2O_3 content (6.08 wt%) measured in orthopyroxene is documented in kelyphitic rims of this lithotype. The content of alumina significantly drops (~ 3 wt%) in texturally equilibrated orthopyroxene as well as in orthopyroxene rims developed around clinopyroxene. Notwithstanding the overwhelming kelyphitization garnet is considered to have attained the peak equilibrium with amphibole and plagioclase. This is corroborated by the numerous and intact inclusions present in garnet porphyroblasts. Amphibole is marked by distinctive pleochroism with a composition ranging from edenite to pargasite (Table 3; Fig. 7b). It has been texturally equilibrated with clinopyroxene with whom it commonly

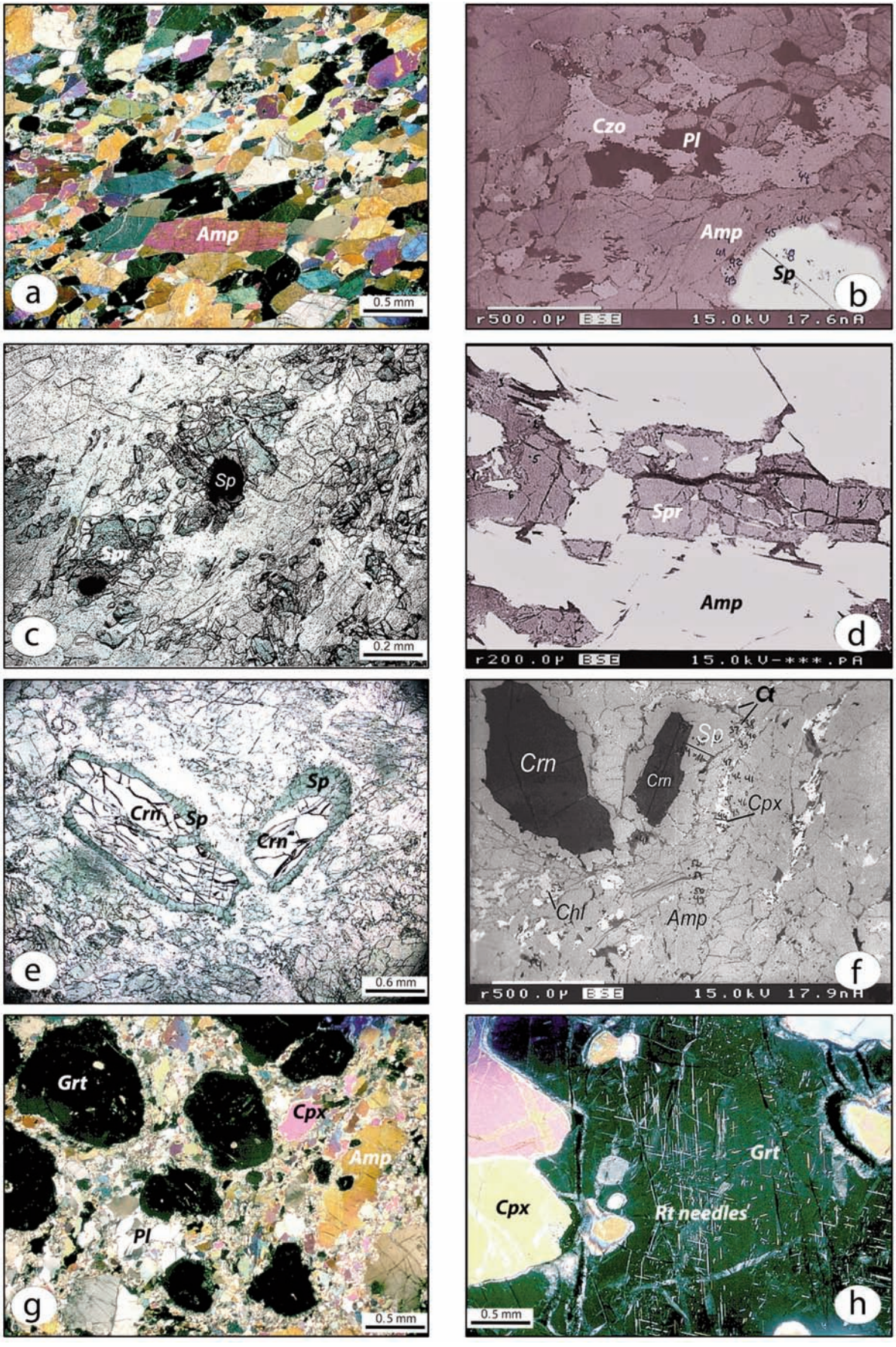

Fig. 6 - Selected microphotographs (crossed nicoles, (a), (g), (h), (n); parallel nicoles, (c), (e), (l), (m), (p)), and BSE images ((b), (d), (f), (i), (j), (k), (o)) of analyzed metamorphic sole rocks. For details see the text; Spr- sapphirine; Sp- spinel; Crn- corundum; Ct- clintonite; Cpx- clinopyroxene; Chl- chlorite; Amp- amphibole; Ttn- titanite; Ilm- ilmenite; Ap- apatite; Pl- plagioclase; Grt- garnet; Rt- rutile; and Opx-orthopyroxene. Mineral abbreviations after Kretz (1983).

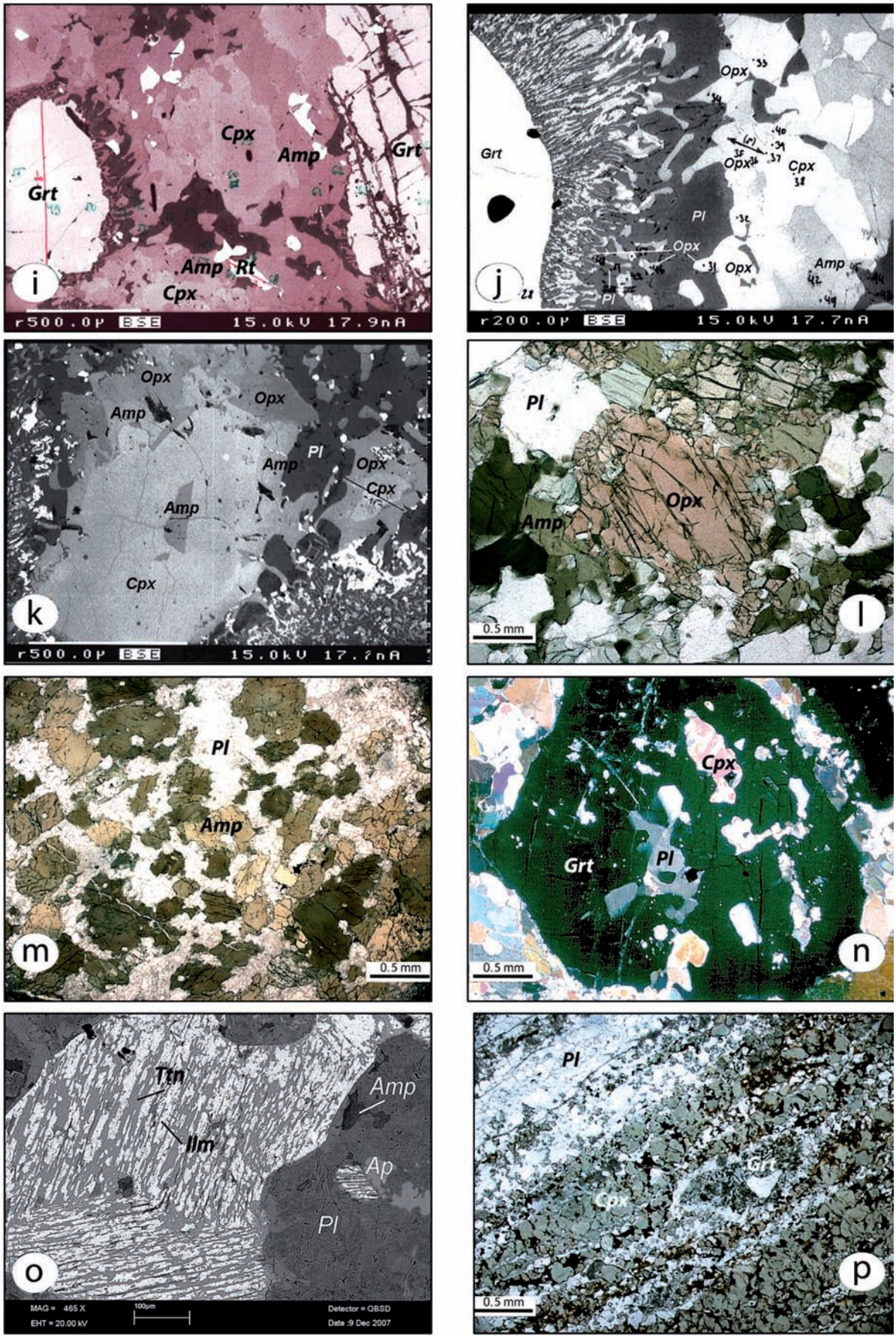

Fig. 6 (*continued*)

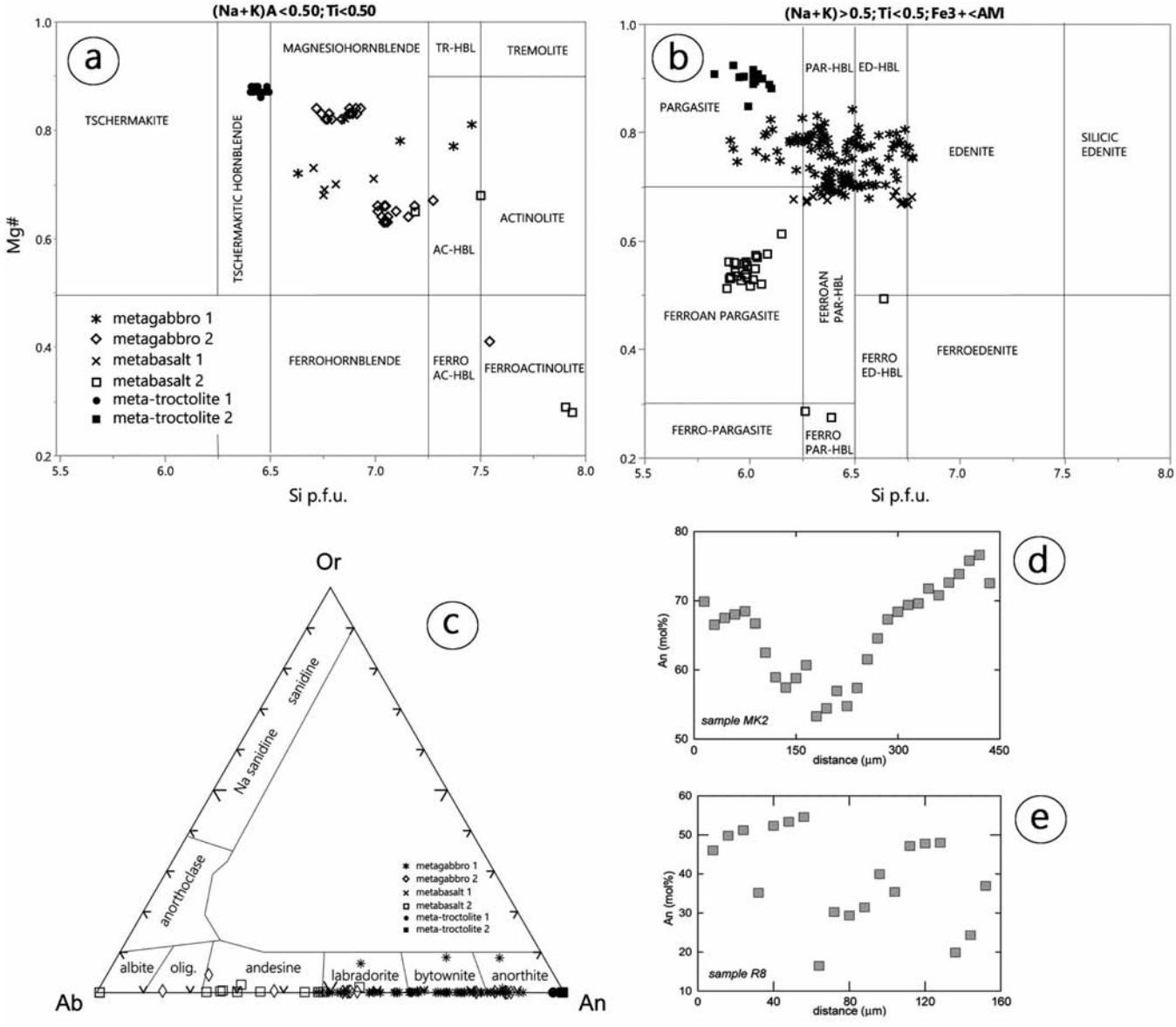

Fig. 7 - (a) and (b) Discrimination diagram for classification and nomenclature of calcium amphiboles (Leake et al., 1997), (c) Ab-Or-An classification diagram for feldspar (Deer et al., 1996), (d) and (e) Compositional line profiles showing An content in plagioclase, in mol% (100*Ca/(Ca+Na+K)).

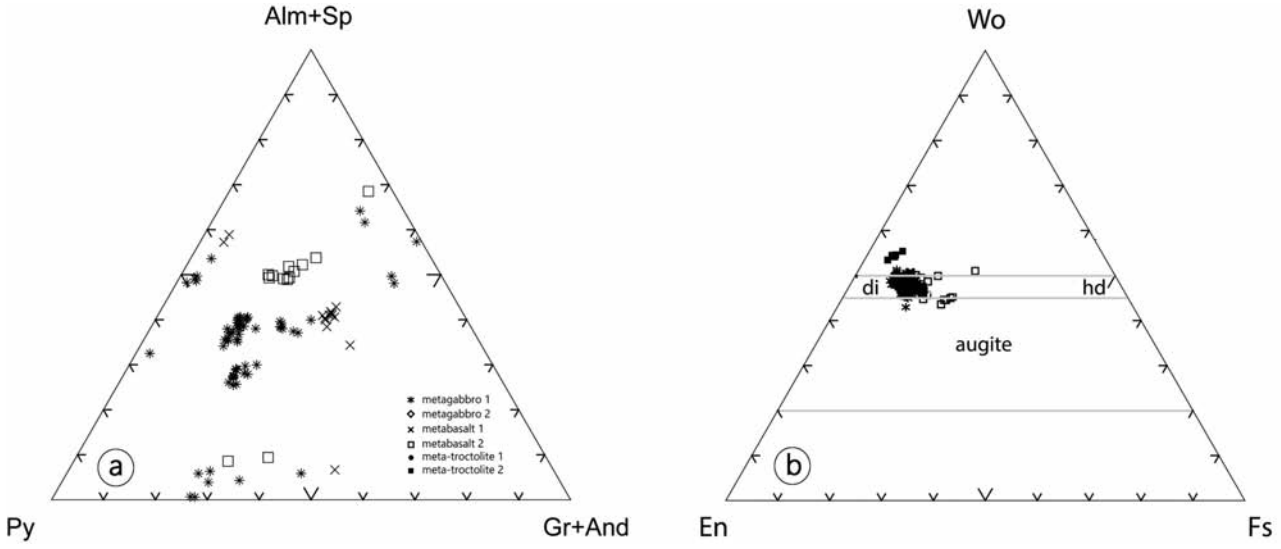

Fig. 8 - (a) Garnet discrimination diagram based on the content of almandine+spessartine (Alm+Sp), pyrope (Py), and grossular+andradite (Gr+And) molecular end-members, (b) clinopyroxene discrimination diagram after Morimoto (1988).

Table 3 - Selected electron microprobe analyses (in wt%) of amphibole, garnet, and plagioclase feldspar from KKOC soles and respective structural formulas.

Rock variety	MT	MG	MG	MG	MG	MG	MG	MB	MG	MG	MB	MT	MG	MG	MG	MB
Sample	U29	R8	CC1	U22	U40	10D	GR7	DU5	V1	V4	Z1C	U29	R8	MK2	V1	Z1C
No. anal.	56	23	13	13	8	47	28	2	102	28	1	45	4	29	87	49
Mineral	Am	Am	Am	Am	Am	Am	Grt	Grt	Grt (kel.rim)	Grt	Grt	Pl	Pl	Pl	Pl (in Grt)	Pl
SiO_2	40.28	49.64	44.42	40.76	43.14	39.9	40.64	39.41	37.09	40.79	37.73	42.44	53.25	46.52	50.53	58.94
TiO_2	0.12	0.18	0.77	0.09	1.52	2.32	0.03	0.09	0.03	0.03	0.14	-	-	-	-	-
Al_2O_3	18.45	3.8	11.42	16.76	12.2	13.71	21.77	22.11	21.4	22.7	21.08	36.58	29.36	34.69	31.49	26.24
Cr_2O_3	0.62	0	0.1	0.2	0.03	0.09	0.12	0.11	0.2	0.15	0.05	-	-	-	-	-
Fe_2O_3	-	-	-	-	-	-	0.899	0.98	17.28	0	3.3	0.11	0.29	0.29	0.32	0.3
FeO	4.92	22.26	12.27	9.98	11.24	16.21	13.17	18.53	0.9	15.72	21.94	-	-	-	-	-
MnO	0.05	0.36	0.17	0.36	0.15	0.2	0.14	0.66	1.2	0.79	2.17	-	-	-	-	-
MgO	15.48	8.42	13.74	14.76	14.17	9.86	13.87	7.19	22.58	13.51	5.58	-	-	-	-	-
CaO	13.19	12.11	11.21	11.27	11.24	11.7	8.26	11.84	0.19	6.26	8.64	20.48	11.74	17.1	13.94	7.42
Na_2O	2.7	0.25	2.08	3.33	2.52	2.91	-	0.01	0	0.19	0.16	0.01	5.14	1.87	3.71	7.62
K_2O	0.69	0.06	0.06	0.01	0.03	0.17	0.02	0	0	0	0	0	0.04	0.01	0.01	0.04
H_2O	3.8	2.95	3.76	2.49	3.76	2.93	-	-	-	-	-	-	-	-	-	-
Total	96.2	97.05	96.24	97.51	96.24	97.07	99	100.91	100.87	99.97	100.66	99.65	99.82	100.48	100.01	100.56
Si	5.83	7.55	6.6	5.91	6.38	6.06	3.02	2.98	2.62	3.01	2.93	1.98	2.42	2.13	2.3	2.62
Ti	0.01	0.02	0.09	0.01	0.17	0.26	0	0.01	0	0	0.01	-	-	-	-	-
Al	3.1	0.68	1.99	2.86	2.12	2.45	1.9	1.97	1.78	1.98	1.93	1.02	1.57	1.88	1.69	1.38
Cr	0.07	0	0.01	0.02	0	0.01	0	0.01	0.01	0.01	0	-	-	-	-	-
Fe^{3+}	0.26	0.1	0.08	0.34	0.04	0.01	0.05	0.06	0.97	0	0.19	0	0.01	0.01	0.01	0.01
Fe^{2+}	0.34	2.72	1.43	0.87	1.35	2.05	0.82	1.17	0.05	0.97	1.43	-	-	-	-	-
Mn	0.01	0.04	0.02	0.04	0.02	0.03	0.01	0.04	0.07	0.05	0.14	-	-	-	-	-
Mg	3.34	1.91	3.03	3.19	3.13	2.23	1.53	0.81	2.48	1.49	0.65	-	-	-	-	-
Ca	2.05	1.97	1.78	1.75	1.78	1.9	0.66	0.96	0.01	0.5	0.72	1.02	0.57	0.84	0.68	0.35
Na	0.76	0.07	0.6	0.94	0.06	0.86	0	0	0	0	0	0	0.45	0.17	0.33	0.66
K	0.13	0.03	0.01	0	0	0.03	0	0	0	0	0	0	0	0	0	0
OH	2	2	2	2	2	2	-	-	-	-	-	-	-	-	-	-
Mg#	90.1	41.2	67.8	78.5	69.8	52.1	63.87	39.76	70.78	60.5	28.56	-	-	-	-	-
Py	-	-	-	-	-	-	50.82	27.16	94.71	49.53	22.04	-	-	-	-	-
Gr	-	-	-	-	-	-	18.72	28.8	0	16	14.59					
An	-	-	-	-	-	-	-	-	-	-	-	99.9	55.6	83.4	67.4	34.9

Chemical analyses of most minerals performed with focused electron beam of approx. 1 mm radii. Feldspar measured by electron beam of 10 mm. Fe analysed as FeO_{total} and estimated as Fe^{2+} and Fe^{3+} on fixed number of 8 cations/12 oxygens for garnet and 15 cations/23 oxygens for amphibole. Formulas of plagioclase calculated on the basis of 8 oxygens, FeO_{total} is expressed as Fe_2O_3. Mineral abbreviation (Kretz, 1983): Am = amphibole, Grt = garnet and Pl = plagioclase, Py = pyrope, Gr = grossulare, An = anorthite (all in %), Mg#=Mg/(Mg+Fe^{2+}), kel.rim = kelyphitic rim. MT- meta-troctolite; MG- metagabbro; MB- metabasalts.

Table 3 (*continued*)

Rock variety	MT	MB	MG	MG	MG	MG	MB	MG	MG	MG	MT	MG	MT	MT	MT	MB
Sample	U29	11C	CC1	V1	U40	V4	Z1C	MK2	V1	U40	U30	U23	U30	U29	U29	Z1C
No. anal.	62	23	70	60	16	22	23	47	101	64	29	23	1	4	6b	62
Mineral	Cpx	Cpx	Cpx	Cpx (in Am)	Cpx	Cpx	Cpx	Opx (cpx.r)	Opx (k.rim)	Opx (k.rim)	Czo	Prh	Spr	Al-Sp	Cr-Sp	Usp
SiO_2	48.18	53.02	52.43	51.47	50.73	53.61	50.18	53.75	51.36	50.57	39.34	43.28	13.05	-	-	0.15
TiO_2	0.49	0.04	0.41	0.1	0.37	0.05	0.46	0.11	0	0.05	0	0.06	0	0	0	15.03
Al_2O_3	8	1.04	9.03	3.15	4.14	1.56	3.38	2.13	5.21	6.08	32.84	24.47	64.79	66	55.42	1.13
Cr_2O_3	0.52	0.05	0.07	0.03	0.03	0.04	0	0.07	0.014	0.18	0	0.06	0.1	0.41	10.51	0.24
Fe_2O_3	-	-	-	-	-	-	-	-	-	-	-	-	-	-	-	-
FeO	2.86	6.9	4.91	6.53	7.34	5.09	8.34	15.5	14.73	16.3	0.19	0.28	3.96	13.59	19.12	75.98
MnO	0.07	0.24	0.1	0.17	0.26	0.23	0.31	1.47	1.26	0.79	0	0.04	0.09	0.33	0.45	0.51
MgO	13.55	14.19	11.07	14.84	13.91	16.02	13.75	26.71	26.48	25.44	0	0.02	18.65	19.26	13.66	0.09
CaO	25.32	24.13	19.43	21.58	22.45	23.3	21.63	0.69	0.29	0.33	24.56	26.89	0.05	0.05	0.31	0.08
Na_2O	0.03	0.35	2.21	0.5	0.59	0.35	0.64	0	0	0.01	0.06	0.01	0	-	-	0.02
K_2O	0	0	0.04	0	0	0	0	0	0	0.01	0	0.02	0	-	-	-
H_2O	-	-	-	-	-	-	-	-	-	-	3.02	4.88	-	-	-	6.77
Total	99.01	99.95	99.7	98.37	99.82	100.26	98.68	100.42	99.34	99.75	96.98	95.12	100.87	99.69	99.83	93.23
Si	1.78	1.96	1.9	1.92	1.88	1.96	1.88	1.93	1.86	1.83	3.01	2.99	1.51	-	-	0.01
Ti	0.01	0	0.01	0	0.01	0	0.01	0	0	0	0	0	0	0	0	0.44
Al	0.35	0.05	0.38	0.14	0.18	0.07	0.15	0.09	0.22	0.26	2.96	1.99	8.84	1.97	1.77	0.05
Cr	0.02	0	0	0	0	0	0	0	0	0.01	0	0	0.01	0.01	0.23	0.01
Fe^{3+}	0.05	0.05	0	0.05	0.09	0.04	0.11	0.03	0.07	0.07	0.01	0.02	0.13	0.02	0.01	1.05
Fe^{2+}	0.04	0.17	0.15	0.16	0.14	0.12	0.16	0.43	0.38	0.42	0	0	0.26	0.26	0.42	1.42
Mn	0	0.01	0	0.01	0.01	0.01	0.01	0.05	0.04	0.02	0	0	0.01	0.01	0.01	0.02
Mg	0.75	0.78	0.6	0.83	0.77	0.87	0.77	1.43	1.43	1.37	0	0	3.22	0.73	0.55	0.01
Ca	1	0.96	0.76	0.86	0.89	0.91	0.87	0.03	0.01	0.01	2.01	1.99	0.01	0	0.01	0
Na	0	0.03	0.16	0.04	0.04	0.03	0.05	0	0	0	0.01	0	0	-	-	0
K	0	0	0	0	0	0	0	0	0	0	0	0	0	-	-	0
OH	-	-	-	-	-	-	-	-	-	-	1	1	-	-	-	-
Mg#	95	82.5	80.1	84	84.7	88	83.2	76.8	79	76.6	-	-	92.6	73.3	56.6	0.4
Wo	54.5	48.8	50.1	45.5	47	46.8	45.5	1.3	0.6	0.7	-	-	-	-	-	-
En	40.6	39.9	39.8	43.5	40.5	44.8	40.3	72.7	74.2	72.1	-	-	-	-	-	-
Fs	4.9	0.8	10.1	11	12.4	8.3	14.2	25.9	25.2	27.2	-	-	-	-	-	-

Table 3 (*continued*)

Rock variety	MG	MG	MB	MT
Sample	U40	CC1	10D	U29
No. anal.	60b	25	45	8
Mineral	Mt	Ilm	Tit	Ct
SiO_2	1.47	0	30.16	15.64
TiO_2	0.14	53.36	38.1	0.05
Al_2O_3	1.24	0	1.04	44.62
Cr_2O_3	0.17	0.06	0	0.09
Fe_2O_3	-	-	-	-
FeO	88.2	42.87	0.62	2.39
MnO	0	0.02	0.01	0
MgO	0.33	2.31	0.01	18.36
CaO	0.23	0.1	28.49	12.89
Na_2O	0.02	0	0.02	0.26
K_2O	0	0	0.01	0
H_2O	-	-	-	4.2
Total	91.81	98.96	98.45	94.3
Si	0.06	0	1	1.12
Ti	0	1	0.95	0
Al	0.06	0	0.04	3.76
Cr	0.01	0	0	0.01
Fe^{3+}	1.82	0	0.02	0.04
Fe^{2+}	1.03	0.9	0	0.11
Mn	0	0.01	0	0
Mg	0.02	0.09	0	1.96
Ca	0.01	0	1.01	0.99
Na	0	0	0	0.04
K	0	0	0	0
OH	-	-	-	2
Mg#	1.8	8.8	-	94.8

comes up in an intimate contact (Fig. 6i). Clinopyroxene is a high-Al diopside (Table 3; Fig. 8b) typically marked by a faint coloration. Rarely, the clinopyroxene is found resorbed in amphibole which may indicate its relict nature. More common are, however, the thin rims of amphibole and orthopyroxene developed around clinopyroxene (Fig. 6k). They are presumably formed during decompression, coevally with the development of garnet coronas, as a result of incomplete re-equilibration of high-grade metamorphic assemblages (e.g. Groppo et al., 2015). Plagioclase occurs in the form of small polygonal interstitial grains and only exceptionally it emerges in the form of larger blasts. It is relatively calcic (labradorite to anorthite, Fig. 7c) and devoid of alterations. The zoning of plagioclase shows a "U"-shape An content which is prevalent in high-grade metabasites (Fig. 7d). Small euhedral grains (up to 0.05 mm in size) of brown rutile and black ilmenite are reported to be ubiquitous in this rock type. They are considered to be a part of the peak high-pressure paragenesis (e.g. Meinhold et al., 2008), or alternatively they may form during decompression and cooling in case of a Ti-rich igneous protolith (Finger et al., 2003). The second subgroup of this rock type is characterized by the texturally equilibrated orthopyroxene that is known to occur in the form of pinkish pleochroitic crystalloblasts (Fig. 6l). Orthopyroxene may occasionally include the lobate and xenomorphic grains of amphibole.

Amphibolite (metagabbro 2)

rock type is characteristic for central and southern areas of KKOC (Maoče and Dubоštica, Table 1). Mineral assemblage of this rock type is consisted of hornblende and plagioclase whereas titanite, prehnite, ilmenite, chlorite, and apatite are present as minor phases (Table 2). The lobe-shaped amphibole (up to 2 mm in size) limn the amphibolite granoblastic texture (Fig. 6m). The equidimensional grains and common triple junctions connote that the peak metamorphism textural equilibrium among amphibole, plagioclase and minor phases was attained. The xenomorphic grains of plagioclase readily fill the amphibole interstitial space, which is indicative for the relic igneous cumulate textures (e.g. Gartzos et al., 2009). Amphibole is the fresh and green magnesiohornblende that is only sporadically altered into secondary ferroactinolite (Table 3; Fig. 7a). Plagioclase is of intermediate, andesine to labradorite composition (Fig. 7c). The variations in plagioclase chemistry are manifested by a pronounced oscillatory zoning of anorthite content (Fig. 7e). This, however, may be a legacy of its igneous origin (e.g. Rutland and Sutherland, 1968). Due to the inconsistency in plagioclase chemistry this rock type was not considered for geothermobarometric calculations. Titanite is the most abundant accessory mineral usually found incorporated in hornblende in the form of ellipsoidal blebs. The average composition of titanite is uniform across the all KKOC sole lithotypes corresponding to the average composition of $Ca_{0.982\text{-}1.014}(Ti_{0.882\text{-}0.965}Fe^{3+}_{0.013\text{-}0.044}Al_{0.036\text{-}0.118})SiO_5$, which indicates a low $(Al, Fe^{3+}) + (OH^-, F^-) \leftrightarrow Ti^{4+} + O^{2-}$ substitution (Higgins and Ribbe, 1976).

Cpx±Grt amphibolite (metabasalts 1)

has been recovered from the central and north-western portion of the complex (samples 11C and DU5; Table 1). Major phases in this rock type are amphibole, plagioclase, clinozoisite, clinopyroxene while ilmenite, titanite, chlorite, prehnite, apatite, albite and Fe- to Al- pumpellyite emerge as minor phases (Table 2). Garnet is a member of the primary paragenesis in the sample DU5 with plagioclase occurring solely as inclusions in garnet. The granoblastic texture of the sample 11C is relic gabbroic defined by the polygonate amphibole blasts (up to 0.4 mm in size). The interstitial space is filled by plagioclase, which is largely sassuritized. Amphibole is the green magnesiohornblende to pargasitic and edenitic hornblende Fig. 7a) marked by a strong pleochroism. Bleb-shaped titanite inclusions in amphibole are commonly reported. Plagioclase alteration products include clinozoisite and prehnite rich aggregates. Prehnite composition is stable in all the analyzed aggregates, whilst clinozoisite is the Fe-poor variety (Table 3). Plagioclase obliteration precluded one to determine if it attained the equilibrium with neighbouring phases. For the same reason this rock type was excluded from geothermobarometric calculations. Amphibole, however, is well equilibrated with garnet and is frequently found enclosed in it (Fig. 6n). Clinopyroxene is diopside (Table 3) occurring only rarely, mostly as a mantle around amphibole. It has the lowest Al_2O_3 content amongst all the clinopyroxene of the complex (~ 2 wt% in the rims and ~ 0.5 wt% in the cores). Ilmenite forms larger blasts (up to 0.4 mm in size) that are usually featured by titanite exsolutions (Fig. 6o). Texture of the sample containing garnet granoblasts (sample DU5) is analogue with the rest of the group and is largely dominated by the polygonate amphibole. Garnet kelyphitic coronas are barely developed containing solely minute patches of xonotlite.

Cpx+Pl± Grt gneiss (metabasalts 2)

is known from the western segment of the Krivaja-Konjuh ophiolite complex (samples 10D and Z1C; Table 1).

Similarly to Cpx±Grt amphibolite this rock type is either devoid (sample 10D) or it includes garnet blasts (sample Z1C; Table 2). The former is consisted of amphibole, clinopyroxene and altered plagioclase while accessory phases are titanite, ilmenite, apatite and prehnite. Metamorphic texture is granoblastic with alternating enrichment of amphibole and clinopyroxene which creates an apparent layering of amphibole and clinopyroxene rich bands. Amphibole is characterized by a brownish colour and expressed pleochroism (ferrous pargasite; Fig. 7a). Its TiO_2 and Al_2O_3 contents are somewhat elevated (~ 4.1 and 14.8 wt%, respectively) which appears to be typical for Ti-rich pargasite (i.e. kaersutite) from high-grade metabasalts from sub-ophiolitic metamorphic soles (Raase et al., 1986). The Mg#-impoverished amphibole is also documented (Fig. 7a) forming at the expense of the primary pargasite and clinopyroxene. Clinopyroxene emerges as a pale green blasts having no pleochroism. Its chemistry corresponds to diopside and augite (Fig. 8b). Despite a completely obliteration of plagioclase one may still reconstruct its xenomorphic habits. Sample with garnet (Z1C) further contains clinopyroxene and plagioclase, while orthopyroxene, titanite, ilmenite, and ulvöspinel are minor phases (Table 2). Rock's gneissic nature is defined by the alternation of brownish bands rich in clinopyroxene and lens-shaped domains largely consisted of plagioclase (Fig. 6p). Pale-green clinopyroxene has a distinct augite chemistry (Fig. 8b). It is characterized by a somewhat higher Fe and Na content p.f.u. compared to clinopyroxene from other sole lithotypes (Table 3). Epitaxial orthopyroxene that encloses clinopyroxene is commonly reported. Relatively small pinkish porphyroblasts of claw-shaped garnet are found in the clinopyroxene-rich bands. Garnet kelyphite rims are ubiquitous but are barely developed. Ilmenite, titanite, plagioclase, clinopyroxene and apatite are readily found engulfed in garnet. The dominant opaque phase is a xenomorphic ulvöspinel found in a close but texturally dis-equilibrated contact with clinopyroxene. Andesine plagioclase (Fig. 7c) occurs as an anhedral, granular to rod-shaped crystalloblasts (~ 0.5 mm in size), free from twinning. Similar sole rocks were documented elsewhere in the Dinarides and are suggested to represent a transitional facies toward eclogite metamorphic conditions (Pamić et al., 1973).

Whole-rock geochemistry

The complete data-set of whole-rock ICP-MS measurements of the KKOC metamorphic soles is provided in Table 4. Major element geochemistry is marked by the SiO_2 content that lies in the range from 39.70 to 50.10 wt%, MgO from 8.36 to 20.00 wt%, and Al_2O_3 from 12.61 to 27.47 wt%. Extremely high Al_2O_3 and MgO end-values significantly deviate from their mean abundances (16.55 and 11.38 wt% respectively) due to the unique mineralogy of the respective samples (i.e. Crn-bearing and Spr-bearing amphibolite). Iron is found in a broad range from 7.70 to 14.50 wt%. The CaO ranges from 9.12 to 19.30 wt% and alkalis cover a large span with Na_2O and K_2O spreading from 1.11 to 3.67 and 0.02 to 0.29 wt%, respectively. The Cpx+Pl±Grt gneiss has apparently higher TiO_2 concentrations (1.34 and 2.21 wt%, respectively) compared to other rock varieties (0.49 wt%, mean value). Apart from TiO_2, the P_2O_5 content in Cpx+Pl±Grt gneiss is on average 10 times higher (0.13 and 0.19 wt%, respectively) compared to the rest of dataset (0.05 wt%, mean value). Such high Ti and P proportions and their positive correlation are best explained through the accumulation of apatite and ilmenite (Gómez-Pugnaire et al., 2003). Higher amounts of those minerals in addition to other Ti-phases such as titanite and ulvöspinel are reported in the KKOC gneiss (Table 2). Overall geochemistry consistently shows that most of the KKOC soles is of clear tholeiitic affinity. This is best depicted by the HFS element ratios of Nb/Y vs. $Zr/(P_2O_5*10000)$ (Fig. 9a). Plausible protoliths of analyzed rocks, based on the ratio of its main elements (TiO_2 vs. Mg#), are defined as low to high-Ti basalts (Fig. 9b). When Mg-number values exceed 70, the potential protolith is assumed to have a mafic to ultramafic cumulate origin. Meta-cumulates often retain relict magmatic gabbro (ophitic) textures (e.g. samples U23, X1, and U40). The ultramafic affinity of meta-cumulates is corroborated by low abundances of SiO_2 (39.70-48.21 wt%), TiO_2 (0.06-0.55 wt%), FeO (~ 6 wt%), along with comparatively higher MgO values (9.35-20.00 wt%). On the other hand, the samples with the affinity of metabasalts are depleted in MgO (under 9 wt%), whilst FeO content remains high (over 8 wt%). The main element geochemistry of KKOC soles generally corresponds to those of well-documented gabbros and basalts from the Alpine, Corsican and Ligurian ophiolite complexes (e.g. Beccaluva et al., 1980; Serri and Saitta, 1980; Bertrand et al., 1987).

The concentrations of trace elements in analyzed rocks are controlled by the protolith geochemical affinities. In meta-cumulates, concentrations of compatible elements show high ranges, spanning from 35.2 to 269.0, 30.4 to 53.7, and 41 to 257 ppm for Ni, Co and V respectively (Table 4). Concentrations of incompatible elements, such as Zr, Y or Ba, are significantly lower with respect to their abundances in metabasalts. Soles with the basaltic geochemical affinity tend to be enriched in all incompatible elements, especially REEs, Y (18.9-45.8), Zr (25.1-100.4) and Ba (18-201). The chondrite-normalized REE patterns of analyzed rocks are shown in Fig. 10a-b. "Meta-troctolites and metagabbro 1" are characterized by parallel to sub-parallel compositional curves, which is characteristic for the rocks of common origin. Most of the curves exhibit slightly depleted LREE patterns ($(La/Yb)_N$ = 0.12-0.47). Relative impoverishment of Ce is attributed to the early fractionation of the LREE rich minerals such as apatite. The HREE plots are flat ($(Tb/Yb)_N$ = 0.79-1.47), which have a substantial positive Eu anomaly (Eu/Eu* = 1.29-3.02). Moderate LREE depletion and flat HREE patterns account for a somewhat depleted mantle source devoid of residual garnet (e.g. Wood and Banno, 1973; Wankang et al., 1993). In spider diagram normalized to primitive mantle (not shown) negative anomalies of Ti and Nb, as well as positive of Pb, Sr, K and P are documented. Titanium and Nb anomalies define rocks' calc-alkaline character whereas high Sr and K are due to the plagioclase-rich nature of meta-cumulates, but could also reflect metasomatic or metamorphic processes that mobilized LIL elements. The phosphorous positive anomaly may be attributed to the accumulation of accessory apatite (e.g. Thy, 2003). The REE patterns of metabasalts and metagabbro 2 are flat, attaining higher concentration levels that are up to 20 times that of chondrite (Fig. 10a-b). The LREE depletion is less pronounced ($(La/Yb)_N$ = 0.27-0.82), while all samples show a weak negative Eu anomaly (Eu/Eu* = 0.86-0.97). Such fractionated REE patterns are consistent with low degrees of partial melting (N-MORB). Primitive mantle normalized concentrations exceed the standard for up to 1000 times

Table 4 - ICP-MS chemical analyses of high-grade metamorphic soles from the Krivaja-Konjuh ophiolite complex. Values are in wt% (oxides) and ppm (elements).

Sample	U30	U29	11C	R8	U23	CC1	MK2	GR7	V1	DU5	U22	X1	U40	V4	10D	Z1C
SiO_2	41.99	39.7	47.32	50.1	46.05	48.21	47.13	46.31	47.39	41.67	45.38	47.89	47.59	45.21	42.65	45.57
TiO_2	0.09	0.06	0.64	0.92	0.22	0.55	0.48	0.28	0.27	1.26	0.31	0.44	0.4	0.24	1.34	2.21
Al_2O_3	17.71	27.47	15.07	14.88	15.97	16.91	14.76	17.53	15.26	15.37	16.04	14.4	14.02	16.19	12.61	13.12
Cr_2O_3	0.72	0.26	0.04	0.06	0.14	0.07	0.05	0.1	0.05	0.06	0.12	0.06	0.06	0.08	0.03	0.01
FeO	5.08	2.69	8.45	8.38	4.99	6.44	7.93	5.74	7.32	11.21	5.55	7.94	8.3	7.07	10.31	14.5
MnO	0.07	0.05	0.12	0.16	0.09	0.09	0.15	0.09	0.18	0.21	0.11	0.16	0.17	0.13	0.2	0.24
MgO	20	9.49	8.64	8.37	13.35	9.35	10.77	10.7	11.75	11.01	12.22	11.53	11.81	13.27	8.44	8.89
CaO	9.12	15.99	13.37	10.12	14.24	13.49	14.04	15.35	13.87	15.02	14.73	13.85	13.58	12.06	19.3	9.45
Na_2O	1.11	1.33	2.58	3.67	1.32	2.69	2.07	1.62	1.6	1.21	1.83	1.84	1.78	2.32	1.4	2.73
K_2O	0.03	0.22	0.19	0.22	0.09	0.04	0.02	0.03	0.03	0.06	0.18	0.03	0.03	0.05	0.07	0.17
P_2O_5	0.02	0.01	0.04	0.17	0.01	0.03	0.03	0.02	0.02	0.09	0.01	0.01	0.02	0.01	0.13	0.19
LOI	2.9	2.1	2.3	1.8	2.7	1.1	1.3	1.3	1.2	1.3	2.6	0.7	0.9	2.3	2.1	1
Total	98.12	99.11	98.72	98.79	99.03	98.9	98.68	98.97	98.89	98.41	98.96	98.79	98.6	98.85	98.55	98.07
Mg#	87.54	86.28	64.57	64.04	82.68	72.12	70.77	76.86	74.11	63.66	79.69	72.14	71.73	77	59.35	52.22
Cs	<0.1	<0.1	1	<0.1	<0.1	<0.1	<0.1	<0.1	<0.1	<0.1	0.2	<0.1	<0.1	<0.1	2.8	2.7
Rb	0.6	2.1	3.3	1.3	0.9	0.4	<0.1	0.5	0.6	0.5	3.5	0.3	0.4	0.2	0.9	3.6
Ba	3	26	201	18	8	8	2	9	3	4	12	1	2	3	24	25
Th	<0.2	<0.2	<0.2	<0.2	<0.2	<0.2	<0.2	<0.2	<0.2	<0.2	<0.2	<0.2	<0.2	<0.2	0.9	<0.2
U	<0.1	<0.1	<0.1	<0.1	<0.1	<0.1	<0.1	<0.1	<0.1	<0.1	<0.1	<0.1	<0.1	<0.1	0.2	0.1
Sr	30.5	333.4	231.7	166.4	112.7	120.9	94.6	121.7	68.4	52.6	182.6	78.3	74.9	80.4	149.2	158.9
Nb	<0.1	0.2	1	2.3	1.1	0.9	<0.1	<0.1	<0.1	2.2	<0.1	<0.4	<0.2	<0.1	<6.3	<5.5
Zr	3.9	1	25.1	59.9	12.8	20.1	6.5	4.3	3.4	52.9	7.5	8.2	5.8	5.6	55.1	100.4
Hf	<0.1	<0.1	0.9	1.7	0.4	0.7	0.2	0.1	0.1	1.4	0.2	0.3	0.1	0.2	1.9	2.8
Pb	<0.1	0.7	0.1	0.3	0.2	0.2	0.2	0.4	0.2	0.1	0.2	<0.1	<0.1	0.1	0.3	0.1
Y	1.9	1.8	18.9	25.6	5.8	11.1	10	6.1	8.6	33.3	6.3	9.8	10.3	5.2	27.8	45.8
Co	63	30.4	44.2	38	43.2	36.3	48.5	40.9	47.1	54.7	37.9	44.4	46.9	53.7	43.8	57.3
Ni	153.8	35.2	35.2	25.1	75.9	34.9	65.5	99.8	69.8	56.7	38.7	51.3	56.1	61.8	60.6	47.8
V	57	41	288	215	103	184	257	167	176	348	183	240	234	122	352	515
Cu	2.6	3.8	46.2	14.8	35.6	49.2	178	119.3	58.9	68.7	40.4	79.3	78.7	73.5	114	106.5
Sc	8	6	39	33	24	33	46	33	43	47	40	47	47	26	45	52
Zn	4	1	8	5	4	7	9	6	6	14	7	5	5	8	25	94
Ga	8.8	11.7	14.1	14.5	9.6	12.4	13.8	13	11.1	14.7	10.9	12.1	12.3	11.9	14	19.3
La	0.3	<0.1	0.9	3.3	1.3	1.8	0.3	0.2	0.4	2.7	0.5	0.2	0.3	0.3	11.9	2.8
Ce	0.8	0.2	2.8	9.4	3.8	4.8	1.2	0.9	0.7	8.6	0.9	0.9	1.1	1.2	27.7	12.3
Pr	0.12	0.04	0.54	1.52	0.53	0.79	0.25	0.21	0.17	1.52	0.19	0.21	0.2	0.22	3.5	2.3
Nd	0.6	<0.3	3.7	8.5	2.1	4.3	1.8	1.4	0.8	8.8	1.2	1.7	1.6	1.3	16.5	13.3
Sm	0.16	0.13	1.52	2.74	0.74	1.58	0.79	0.61	0.55	3.35	0.62	0.64	0.81	0.46	3.95	5.03
Eu	0.17	0.16	0.61	0.98	0.33	0.71	0.5	0.39	0.34	1.21	0.33	0.45	0.44	0.35	1.21	1.69
Gd	0.26	0.21	2.33	3.72	0.87	1.99	1.3	0.91	1	4.86	0.94	1.35	1.3	0.79	4.69	7.23
Tb	0.06	0.04	0.49	0.72	0.16	0.37	0.27	0.18	0.19	0.96	0.2	0.28	0.27	0.15	0.86	1.37
Dy	0.4	0.37	3.27	4.38	1.01	2.08	1.65	1.12	1.53	5.96	1.19	1.85	1.85	0.88	5.19	8.57
Ho	0.06	0.07	0.75	0.97	0.22	0.42	0.37	0.23	0.36	1.34	0.24	0.42	0.41	0.21	1.14	1.96
Er	0.21	0.19	2.36	2.69	0.71	1.16	1	0.64	1.06	3.89	0.76	1.23	1.29	0.66	3.33	5.59
Tm	0.03	0.03	0.38	0.45	0.12	0.17	0.16	0.11	0.16	0.64	0.12	0.2	0.2	0.09	0.53	0.89
Yb	0.18	0.22	2.27	2.71	0.65	1.05	1.05	0.63	1.06	3.84	0.72	1.17	1.24	0.55	3.16	5.32
Lu	0.03	0.03	0.36	0.39	0.1	0.16	0.16	0.09	0.18	0.6	0.1	0.18	0.19	0.08	0.48	0.82

Total Fe as FeO. *Abbreviations*: PGDA- Porphyroblastic garnet-diopside amphibolites, GA- Granoblastic amphibolites, GDHA- Garnet-diopside-hypersthene amphibolites, PGDG- Plagioclase-garnet-diopside gneisses, DAG- Diopside-amphibolite gneisses.

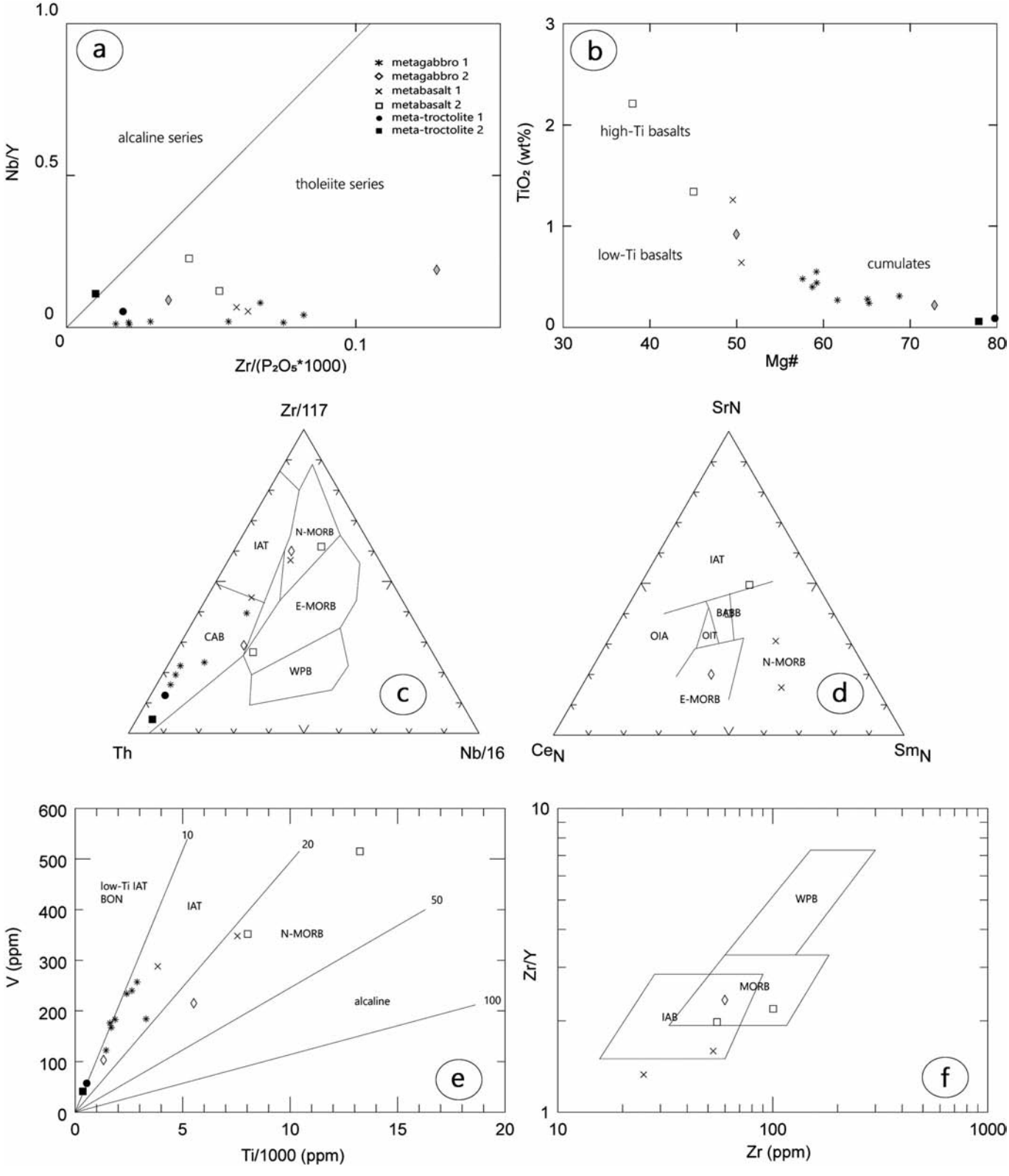

Fig. 9 - (a) $Zr/(P_2O_5*10000)$ vs. Nb/Y discrimination diagram depicting tholeiitic affinity of analyzed rocks (after Floyd and Winchester, 1975), (b) Mg-number vs. TiO_2 diagram showing differences between high- and low-Ti basalts (2 wt% TiO_2 limit). Field of mafic cumulates after Gómez-Pugnaire et al. (2003), (c) Th-Zr-Nb discrimination diagram of Wood (1980), (d) Ce_N-Sr_N-Sm_N diagram of Ikeda (1990), normalized to average chondrite (Ikeda et al., 1981), (e) V vs. Ti variation diagram of Shervais (1982), (f) Zr/Y vs. Zr diagram of Pearce and Norry (1979) for KKOC soles.

(not shown). Weak negative Ti and positive P anomalies are also observed. The REE pattern of sample 10D is analogue to the rest of metabasalts except for the significant LREE enrichment ($(La/Yb)_N$ = 0.84; Fig. 10b). This discrepancy is best explained by a different provenance of this sample, which clearly corresponds to transitional to evolved MOR basalts (Saunders, 1984; Langmuir et al., 1992; McDonough and Sun, 1995).

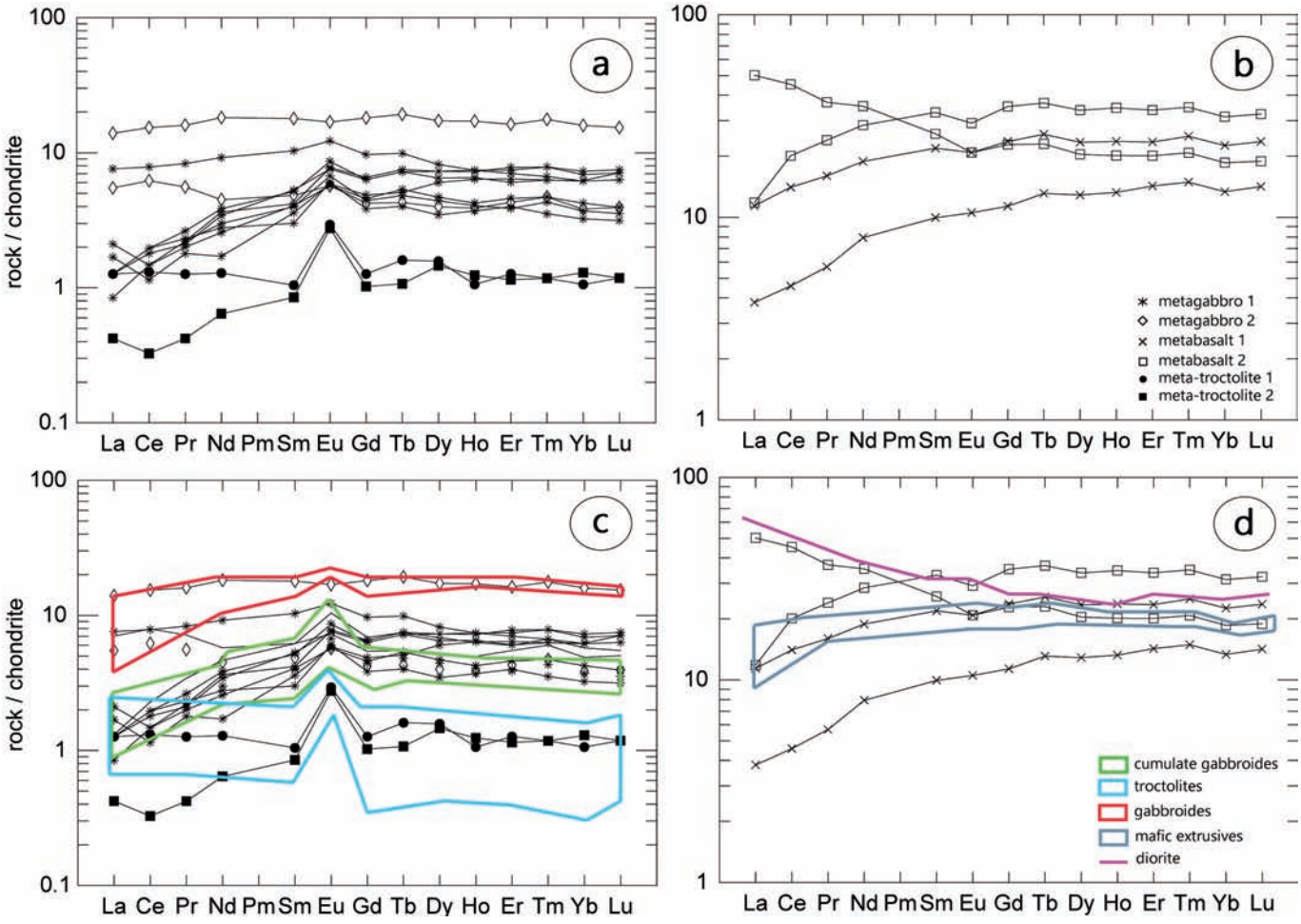

Fig. 10 - Chondrite-normalized abundances of REE in the KKOC metamorphic sole rocks - (a) meta-troctolites and metagabbros and (b) metabasalts. Normalisation values are after McDonough and Sun (1995). Comparison of chondrite-normalized REE patterns with the potential mafic protoliths (KKOC mafic intrusives and extrusives, Babajić (2009), raw data in Table 5). Mafic rocks are marked with lines of different colour. (c) and (d). Normalisation values according to McDonough and Sun (1995). For details see the text.

DISCUSSION

Magmatic protoliths and their original geotectonic setting

As suggested by their respective trace-element geochemistry, the protoliths of the KKOC metamorphic sole rocks can be defined as either mafic to ultramafic meta-cumulates or evolved metabasalts of tholeiitic affinity (Fig. 9b). This is in line with the ratios of incompatible elements La/Sm and Zr/Nb insensitive to magmatic differentiation that show narrow ranges of 0.59 to 1.20 and 18.25 to 26.04, respectively (sample 10D omitted), which is characteristic for normal to transitional MORB (Sun and McDonough, 1989). Ternary discrimination diagrams based on incompatible element concentrations were used to further constrain the geochemical setting of igneous protoliths. In the Th-Zr-Nb plot of Wood (1980) (Fig. 9c), metabasalts are defined as N-MORB, whilst meta-cumulates bear arc-signatures (here CAB). The results of this classification might have been slightly affected by the loss of Zr due to its early fractionation (e.g. Reagan and Meijer, 1984). Metabasalts were additionally considered in the trilinear plot of Ikeda (1990) that takes into account normalized concentrations of Ce-Sr-Sm (Fig. 9d). Therein, analyzed samples are projected as N-MORB, with the exception of sample 10D that fits in the E-MORB field. Meta-cumulates were not considered in this classification scheme due to the impending Sr accumulation. Further classification is based on the V vs. Ti and Zr/Y vs. Zr ratios, where the non-arc affiliation is shown to be strongly corroborated for KKOC metabasalts (Fig. 9e-f), whereas meta-cumulates depict the apparent arc signatures (IAT affiliation, Fig. 9e).

Overall geochemical characteristics define the KKOC meta-cumulates as former igneous rocks formed by silicate accumulation (plagioclase, pyroxene, minor olivine, and ilmenite) best corresponding to shallow ocean-crust gabbroic cumulates (Jaques et al., 1983; Rasool et al., 2015). These rocks must have been influenced by H_2O-rich slab-derived fluids as manifested by Ti and Nb negative anomalies, which in turn defines a hypothetical back-arc basin as their most plausible original geotectonic setting. Conversely, metabasalts display only minor indications of subduction influences reflected in the Ti negative anomaly and somewhat elevated Th content. Their parental magmas are evolved and best correspond to N-MORB-like geotectonic setting. For sample 10D, however, an E-MORB geotectonic setting may be envisaged due to comparatively higher values of Ce, Nb, and Th. Basic geochemical differences of

the KKOC meta-cumulates and metabasalts correspond well to the results of recent investigations on oceanic crust showing that an average upper 500 m gabbro section tends to be impoverished in Ba, Nb, U, and heavy REEs compared to N-MORB, while being somewhat enriched in La, Ce, Pb, and Sr (Hart et al., 1999; Dick et al., 2000; Çelik et al., 2016).

Finally, the KKOC rare-earth element patterns were compared to those of the mafic intrusives and extrusives that originate from the same ophiolite complex (Babajić, 2009; Figs. 10c-d). Hence, the metagabbros shows the best correspondence to cumulate gabbroides (gabbros, gabbronorites to amphibole gabbronorites) and gabbroides that both crop out from the southern and western KKOC (Figs. 2, 10c; Table 5). Meta-troctolites are somewhat different from the rest of metacumulates and are featured by significantly lower REE contents highly resembling to those of troctolites from the south (Figs. 2, 10c; Table 5). The N-MORB-like metabasalts match the composition of the KKOC massive extrusives (dolerites, diabases and pillow basalts, Figs. 2, 10d; Table 5). Lastly, the sample 10D (metabasalts 2) shows certain similarities with diorites from the southern KKOC margins (Figs. 2, 10d; Table 5).

Mineral assemblages and P-T conditions of metamorphism

Thermobarometric data that are based on the composition of the coexisting metamorphic phases from the KKOC soles is provided in Table 6. Coupled with rocks' textural characteristics, these were utilized to infer on the metamorphic history of analyzed rocks. In case of "meta-troctolites" it was not possible to use Amph-Pl based geothermometers due to the high anorthite content in plagioclase. Still, the estimations hinged on Al content in amphibole (Plyusnina, 1982; Schmidt, 1992) provided the values of metamorphic pressures and temperatures of 0.25 to 0.55 GPa and 540-700 °C, respectively (Table 6). The presence of sapphirine and corundum in this rock type (Table 2) is in line with the maximal values of estimated conditions of metamorphism. In silica under-saturated systems the appearance of sapphirine denotes a progressive silification, with a minimum pressure of 0.7 GPa and temperature of 650 °C (Williams, 1984; Gnos and Kurz, 1994). Operta et al. (2003) had reported on a corundum occurrence in pargasitic amphibolites of the Vijaka locality of KKOC (Fig. 2), which formed at temperatures between 620 and 800 °C and pressures of 0.6 to 0.8 GPa. Al-spinel and clintonite that build the rims around corundum formed under changing conditions, which probably reflect higher water activities at moderate P-T conditions that followed the peak metamorphism (Liati, 1988). The occurrence of the minute relicts of magmatic clinopyroxene, texturally disequilibrated with the host pargasite, suggests that Spr and Crn-bearing amphibolites must have only attained the amphibolite-granulite facies transition at ~ 650 °C and ~ 0.75 GPa (Spear, 1980; Abd El-Naby et al., 2008). Conversely, the frequent formation of clinozoisite and pumpellyite is characteristic for retrogressive metamorphic overprint whereby the hydration proceeds after the breakdown of the upper amphibolite or granulite facies assemblages (Ilnicki, 2002). Finally, based on the textural and geochemical clues one may infer that the crystallization of corundum, sapphirine, and clinopyroxene marks the peak metamorphic conditions while a transformation from magnesio-hornblende and/or actinolitic to edenitic hornblende follows a decrease of pressure and temperature values. The occurrence of actinolite, ferroan pargasite, titanite, albite, and epidote is consistent with the greenschist facies re-equilibration at lower P-T (0.2 GPa and ~ 600 °C).

The presence of garnet and rutile in "metagabbros" indicate a minimum pressure of 0.8 GPa no matter of temperature (Table 2; Ernst and Liu, 1998). The appearance of clinopyroxene under such conditions when no texturally equilibrated orthopyroxene is present denotes the peak temperatures of at least 750 to 800 °C (Guilmette et al., 2008). The Amph-Pl based geothermometers yielded the equilibration temperatures for this rock type between 750 to 950 °C, whilst Grt-Cpx and Grt-Amph Fe-Mg exchange thermometers show the slightly elevated temperature values (max ~ 1000 °C; Table 6). The Grt-Cpx-Pl geobarometer provides a pressure range between 0.80 and 1.25 GPa. Complex texture of this rock type is indicative for its multi-stage metamorphic history. Namely, the igneous protolith of this rocks, presumably consisting of clinopyroxene and plagioclase, underwent a high-pressure amphibolite to granulite metamorphism that reached its peak with amphibole consumption and formation of metamorphic clinopyroxene (Mukhopadhyay and Bose, 1994; Bucher and Frey, 2002). Prograde metamorphism is well-documented by pargasitic substitution in amphibole (Fig. 7b). The peak-metamorphism recorded in these rocks obviously did not last long enough to completely use up the amphibole. And yet, the peak metamorphic conditions were sufficient for the growth of garnet at high sub- to super-solidus temperatures (600-800 °C) by reaction of amphibole and plagioclase which are both regularly reported as inclusions in garnet (Wolf and Wyllie, 1993). Garnet blasts are usually devoid of the curved inclusions trails, which suggests that the garnet growth (i.e. peak metamorphism) is post-kinematic to the main deformation. High metamorphic pressures and temperatures suggested for metagabbros (Table 6) were presumably achieved during intraoceanic subduction of Dinaridic Tethys. The retrograde metamorphic processes must have taken place shortly after the peak metamorphism leading to preservation of reaction textures around garnet and clinopyroxene (Fig. 6j; e.g. Brandt et al., 2003). In case of the former kelyphitic rims made of plagioclase, orthopyroxene, and magnetite are usually reported and as for the latter the thin rims of amphibole and orthopyroxene emerge surrounding clinopyroxene. Such microstructures are generally explained by disequilibrium during decompression which is caused by the shortage of fluids thus hampering the re-equilibration of high-grade assemblages (e.g. Cruciani et al., 2012; Groppo et al., 2015). The final retrogression stage in this rock type is characterized by the titanite intergrown with ilmenite (Fig. 6o), which implies that the cooling and decompression at the later stage were accompanied by hydration (Harlov et al., 2006). The formation of xonotlite around garnet can be linked to this late-stage event (Hacker and Mosenfelder, 1996), along with the occurrence of albite, epidote, pumpellyite and prehnite symplectites in plagioclase. For "metagabbros" where orthopyroxene is found in textural equilibrium with neighbouring phases a heating event at moderate pressures that lasted somewhat longer has been envisaged (e.g. D'el-Rey Silva et al., 2007). This is reflected in scantly higher peak metamorphic temperatures (max ~ 1100 °C; Table 6) that gave rise to the crystallization of orthopyroxene blasts (Fig. 6l).

The temperatures estimated for "metabasalts" were in a range from 720 to 1020 °C, whilst the pressures were reported the highest in the KKOC soles spanning from 1.10 to 1.30 GPa (Table 6). Such high pressure conditions that are

Table 5 - Representative ICP-MS geochemical analyses of different types of mafic rocks from the Krivaja-Konjuh ophiolite complex (Babajić, 2009). Values are in wt% (oxides) and ppm (elements). Sampling locations are shown in Fig. 2.

Sample	1-ER8	2-ER21	3-ER7	4-D9	5-ER14	6-DR19	7-D12	8-DR22	9-ER29	10-DR25	11-ER40	12-ER1	13-ER2	14-ER26	15-ER27
Rock type	Tro	Tro	Gab	Gab	Dio	Dol	Dol	Dia	Dia	Spi	Spi	Mga	Dol	d_GN	d_GN
Samp. locality	Gostovići	Maoča	Gostovići	Duboštica	Duboštica	Ribnica	Duboštica	Ribnica	Ribnica	Ribnica	Mitrovići	Ribnica	Ribnica	Konjuh	Konjuh
SiO_2	43.32	41.74	48	47.66	60.59	48.75	45.38	48.98	49.04	45.85	48.42	40.02	48.35	46.45	46.1
TiO_2	0.08	0.05	0.27	1.77	0.35	1.01	1.04	1.14	1.12	1.32	1.42	2.59	1.63	0.11	0.21
Al_2O_3	21.6	15.3	17.87	15.32	19.72	17.06	15.94	12.28	16.3	15.08	13.73	12.57	14.83	16.51	16.23
Cr_2O_3	0.02	0.17	0.06	0.02	0	0.05	0.06	0.05	0.05	0.0.4	0.01	0.01	0.02		
FeO	4.49	5.32	4.6	11.71	2.74	7.94	8.24	8.65	7.74	10.34	8.63	16.11	10.81	4.67	4.76
MnO	0.06	0.07	0.09	0.19	0.04	0.14	0.13	0.17	0.17	0.17	0.17	0.2	0.19	0.08	0.1
MgO	13.14	21.08	10	7.62	1.52	8.29	10.7	9.03	8.6	7.91	6.83	11.18	6.9	14.56	11.63
CaO	10.72	7.02	12.3	11.96	4.41	11.3	11.93	9.8	9.83	10.88	11.07	10.87	10.64	11.51	14.19
Na_2O	1.44	0.98	2.86	2.3	8.4	2.62	2.25	3.04	3.44	3.07	3.79	1.07	3.33	1.84	1.99
K_2O	0.04	0.06	0.18	0.04	0.19	0.07	0.09	0.5	0.24	0.2	0.28	0.07	0.22	0.04	0.04
P_2O_5	0.02	0.01	0.02	0.03	0.1	0.08	0.1	0.08	0.11	0.17	0.17	0.02	0.16	0.01	0.01
LOI	4.4	7.4	3.1	0.1	1.5	1.8	3.1	2.3	2.5	3.8	4	3.5	1.7	3.5	4.1
Total	98.12	99.03	99.29	98.7	99.56	99.36	98.82	98.97	99.09	98.79	98.5	98.2	98.76	99.28	99.36
Mg#	83.91	87.6	79.46	53.01	49.76	65.06	70.34	65.05	66.45	57.7	58.52	55.23	53.23	84.75	81.33
Cs	<0.1	<0.1	0.2	<0.1	<0.1	<0.1	0.4	0.2	0.3	0.2	0.2	<0.1	0.1	<0.1	0.2
Rb	<1.0	<1.0	2	<1.0	3	<1.0	1	8	3	2	3	3	2	<1.0	<1.0
Ba	1	4	21	7	1440	9	212	54	21	18	22	20	23	29	25
Th	<0.05	<0.05	<0.05	<0.05	4.13	<0.05	0.14	<0.05	0.09	0.11	<0.05	<0.05	0.09	<0.05	<0.05
U	<0.02	0.12	0.02	0.06	1.04	0.05	0.08	0.06	0.04	0.2	1.23	0.06	0.15	0.02	0.02
Sr	265	171	181	132	333	146	463	168	169	208	247	170	158	870	712
Nb	<0.2	0.2	<0.2	0.8	16.5	1.8	2.4	0.9	0.9	2.4	2.8	0.4	2.8	0.8	<0.2
Zr	3	4	8	39	141	59	85	62	76	120	91	21	111	11	5
Hf	<0.1	0.1	0.3	1.7	3.6	1.6	1.8	1.7	1.8	3.2	2.4	1.1	3.1	0.4	0.2
Pb	<5.0	<5.0	<5.0	<5.0	<5.0	<5.0	<5.0	<5.0	<5.0	<5.0	<5.0	<5.0	<5.0	5	<5.0
Y	1.1	1.1	7.1	29.2	14.3	20.5	23.4	25.1	23.8	39.4	31.4	30.4	34.9	6.5	4.6
Co	36	69	31	49	7	35	51	37	37	40	41	60	39	28	58
Ni	320	870	140	90	<20.0	130	280	100	140	70	80	70	40	230	720
V	13	19	110	378	52	192	181	212	195	209	326	508	244	40	30
Cu	20	100	90	90	<10.0	100	51	150	90	90	80	<10.0	70	105	85
Sc	n.a.	n.a.	n.a.	n.a.	n.a.	n.a.	n.a.	n.a.	n.a.	n.a.	n.a.	n.a.	n.a.	n.a.	n.a.
Zn	<30	40	8	130	30	80	181	80	70	110	100	100	110	40	30
Ga	10	7	10	20	10	17	15	15	14	18	15	16	17	13	10
La	0.46	0.35	0.35	0.94	24.9	2.16	3.41	1.69	2.17	4.75	3.85	0.57	5.33	1.08	0.18
Ce	0.66	0.88	0.73	3.54	44.6	6.58	10.1	5.66	8.07	14.7	10.8	2.48	15.4	2.62	0.6
Pr	0.14	0.13	0.22	0.8	4.64	1.17	1.56	1.12	1.46	2.51	1.79	0.77	2.51	0.38	0.12
Nd	0.65	0.6	1.49	5.78	14.3	6.28	7.82	6.44	7.82	13.2	9.38	6.03	12.7	1.92	0.83
Sm	0.18	0.18	0.66	2.49	2.58	2.06	2.37	2.29	2.53	4.14	3.02	2.75	3.93	0.61	0.37
Eu	0.29	0.19	0.46	1.34	0.96	0.95	1	1.01	1.06	1.51	1.22	1.2	1.61	0.37	0.29
Gd	0.2	0.16	1.04	4.07	2.38	3	3.23	3.48	3.55	5.97	4.42	4.59	5.42	0.89	0.59
Tb	0.04	0.03	0.22	0.81	0.41	0.59	0.6	0.68	0.65	1.15	0.84	0.93	1.03	0.17	0.13
Dy	0.21	0.18	1.34	5.25	2.25	3.61	3.79	4.33	4.04	7.06	5.46	5.87	6.45	1.08	0.79
Ho	0.04	0.04	0.26	1.1	0.46	0.72	0.79	0.86	0.85	1.42	1.14	1.15	1.27	0.23	0.16
Er	0.11	0.12	0.76	3.29	1.51	2.1	2.38	2.57	2.53	4.11	3.37	3.26	3.85	0.69	0.48
Tm	0.02	0.02	0.11	0.48	0.24	0.31	0.358	0.39	0.36	0.6	0.49	0.47	0.58	0.1	0.07
Yb	0.12	0.12	0.65	2.91	1.66	1.97	2.26	2.44	2.23	3.78	3.04	2.81	3.49	0.62	0.38
Lu	0.02	0.02	0.02	0.44	0.3	0.29	0.36	0.36	0.39	0.56	0.46	0.41	0.52	0.1	0.06

Total Fe as FeO. *Abbreviations*: Tro- troctolites, Gab- isotropic gabbros, Dio- diorites, Dol- dolerites, Dia- diabases, Spi- spilites, Mga- microgabbros, d_GN- dykes of gabbronorites.

Table 6 - Thermobarometric data for the KKOC metamorphic rocks. For analytical uncertainties consult the respective method reference.

Rock type	Grt+Cpx±Opx amp. (metagabbro 1)	Cpx+Pl±Grt gn. (matabasalt 2)	*Spr & Crn amp. (meta-troctolites)*	*Grt+Cpx±Opx amp. (metagabbro 1)*	*Cpx+Pl±Grt gn. (matabasalt 2)*	*Rock type*
GEOTHERMOMETRES (in °C): *(in GPa)*						***GEOBAROMETERS***
AMPH-PL						Al in AMPH
SPEAR (1980)	750 – 800	n.a.	*0.25 – 075*	*0.65 – 1.10*	*0.85-0.90*	*SCHMIDT (1992)*
HOLLAND & BLUNDY (1994)	750 – 950	n.a.				GRT-CPX-PL
GRT-CPX			*n.a.*	*0.80 – 1.25*	*1.10 – 1.30*	*NEW. & PARK. (1982)*
KROGH (1988)	810 – 1025	720 – 1020				GRT-OPX
GRT-OPX			*n.a.*	*0.80 – 1.10*	*n.a.*	*HARLEY & GREEN (1982)*
HARLEY (1984)	720 – 1100	n.a.	*n.a.*	*1.00 – 1.25*	*n.a.*	*NICKEL & GREEN (1985)*
LEE & GANGULY (1988)	770 – 1000	n.a.				OPX-CPX-GRT-PL
GRT-AMPH			*n.a.*	*0.95 – 1.10*	*n.a.*	*PARIA et al. (1988)*
GRAHAM & POWELL (1984)	780 – 980	n.a.				OPX-GRT-PL
KROGH RAVNA (2000)	740 – 940	n.a.	*n.a.*	*0.90 – 1.30*	*n.a.*	*PERKINS & CHIP. (1985)*
TWO PYROXENES						
WELLS (1977) ***°C, GPa)***	830 – 920	n.a.				***GEOTHERMOBAROMETERS (in***
BREY & KÖHLER (1990)	710 – 900	n.a.	*540 – 700* *0.25 – 0.55*	*≥ 650* *≥ 0.40*	*n.a.*	*PLYUSNINA (1982)*

n.a. = not applicable; amp = amphibolite; gn = gneiss. Mineral abbreviations: Amph = amphibole, Grt = garnet, Pl = plagioclase, Cpx = clinopyroxene, Opx = orthopyroxene, Crn = corundum, Spr = sapphirine.

accompanied by a lack of amphibole and occurrence of garnet somewhat richer in Fe may serve as indications of the transitional eclogite facies conditions. This is in line with the literature reporting on the eclogite-type rocks associated with the ophiolites in the Dinaric Alps (Pamić and Majer, 1973). The ubiquitous development of orthopyroxene rims around clinopyroxene follows the discussion from above suggesting an incomplete re-equilibration during decompression. The Ti and Al-poor and Fe-rich secondary amphibole growing at the expense of Ti-pargasite and clinopyroxene is occasionally reported in this rock type thus documenting a post-peak metamorphic instability (~ 0.26 GPa pressure) (e.g. Sen and Oliver, 1981).

Geodynamic significance of metamorphism

The P-T data estimated for the KKOC metamorphic sole rocks, along with their respective mineral assemblages and rock textures are highly comparable with the characteristics of many dismembered dynamothermal soles (e.g. Gjata et al., 1992). The geochemistry of analyzed rocks suggests a two-fold nature of igneous protolith that consists of IAT affiliated meta-cumulates and MORB-like evolved metabasalts of tholeiitic affinity (Fig. 9e). Accordingly, the cumulate gabbroides of Gostovići and Duboštica (Figs. 2, 10c; Table 5) and massive extrusives (dolerites, diabases and pillow basalts) of Ribnica and Duboštica (Figs. 2, 10d; Table 5) are found as the plausible mafic protoliths of the KKOC soles. Such a diverse magmatic suite is usually formed from mantle-derived basaltic melts, in supra-subduction zone (SSZ) environment, as suggested by HFS elements depletion in analyzed rocks (Gill, 2010). The composite geochemical and petrological affinities of igneous precursors (i.e. IAT cumulate vs. MORB-like extrusives) strongly support their metamorphism in an intraoceanic subduction setting of a back-arc geotectonic regime (Lázaro et al., 2013; Šegvić et al., 2016). Many ophiolite complexes with a documented record of metamorphic soles are composed of an analogous mafic series of cumulates and extrusive mafites - especially along the Tethyan belt, for instance in the Dinarides (Croatia, Bosnia, Serbia; Pamić, 1968; Pamić et al., 2002; Šegvić et al., 2016), the Albanides (Gaggero et al., 2009), Oman (Godard et al., 2006), Greece (Pyndos and Othry Zone; Gartzos et al., 2009) and Turkey (Eldivan; Dangerfield et al., 2011). Ophiolite obduction and tectonic emplacement of oceanic lithosphere explain a tectonic mixing of juxtaposed magmatic bodies of different geochemical provenances that served as protoliths of studied rocks (Lázaro et al., 2013). Field textural evidences and petrogenesis of analyzed rocks are a witness to the genetic link between the KKOC soles and prevalent mafic and ultramafic rocks of the complex. This strongly suggests that the KKOC soles can be considered as dismembered metamorphic rocks that originated in a subduction system as a consequence of convergent processes in the vicinity of a back-arc spreading zone where the newly born oceanic lithosphere remained hot (Robertson, 2002; Saccani et al., 2011).

Such defined geotectonic environment corresponds well to the classical models of Boudier et al. (1985) and Boudier et al. (1988) developed for the Tethyan ophiolites of Oman and which are characterized by the metamorphic sole presence. The igneous precursors of KKOC soles are suggested to have belonged to the lower oceanic plate that re-crystallized when over-thrusted by the hot oceanic lithosphere (Fig. 11a). This is in line with metamorphic conditions elucidated for studied rocks with meta-troctolites having attained the amphibolite-granulite facies transition (~ 650 °C and ~ 0.75 GPa) while metagabbros and metabasalts underwent the high-pressure granulite metamorphism (~ 900 °C and ~ 1.00 GPa). Such a regime follows a trajectory model of Peacock et al. (1994) typical for a slow-subducting oceanic crust at a constant shear. Meta-troctolites presumably represent a portion of the lower plate comparatively more distant to the hanging wall which led to somewhat lower values of the

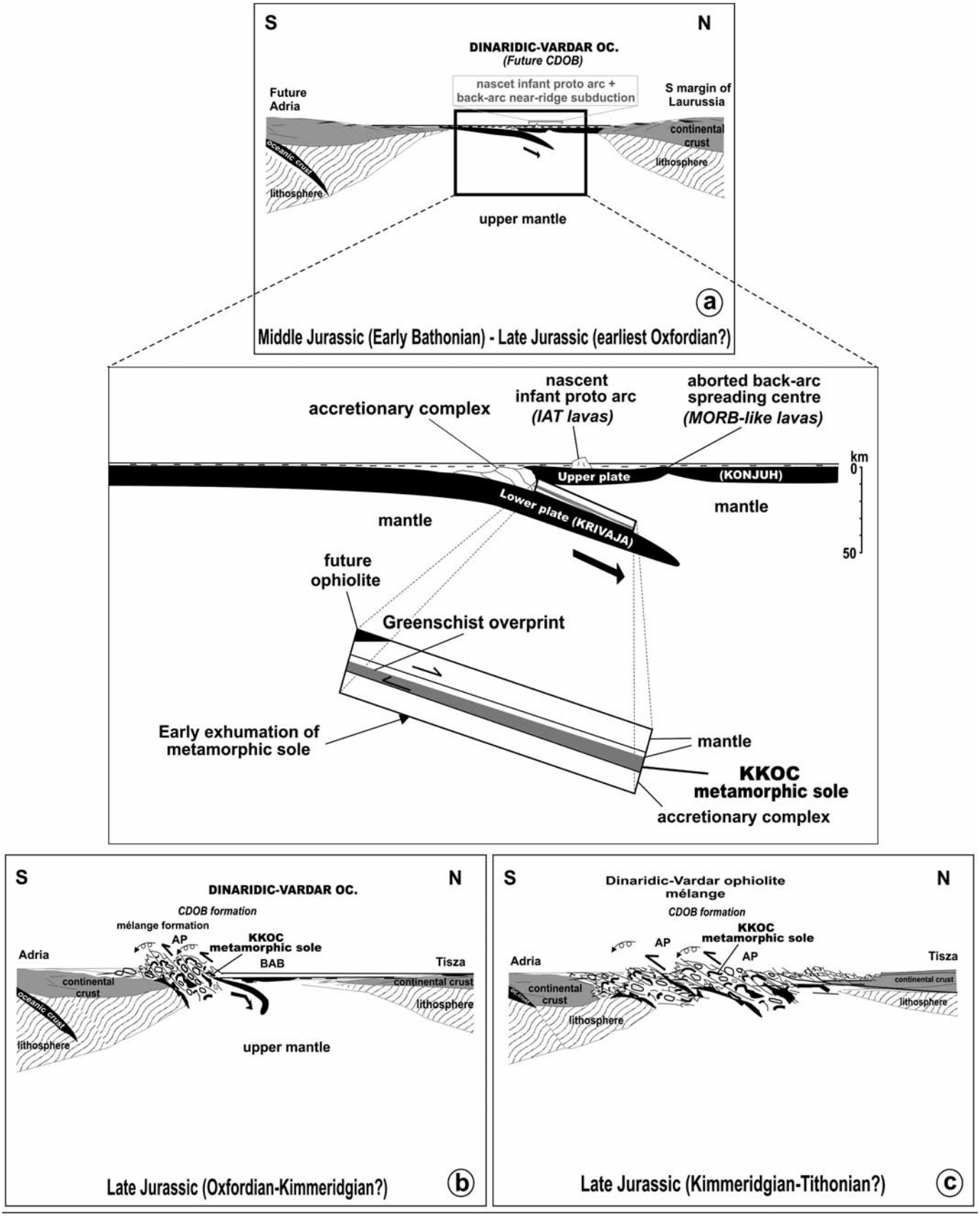

Fig. 11 - The proposed schematic geodynamic model that gave rise to the Krivaja-Konjuh metamorphic sole rocks (dynamothermal soles). (a) The near-ridge subduction stage with formation of an infant proto arc and aborted spreading centre in the marginal (back-arc) basin. Sketch detail: intraoceanic subduction and formation of metamorphic sole and subsequent early exhumation of metamorphic sole relative to the ophiolite (adapted after Wakabayashi and Dilek (2000; 2003). (b) The late subduction stage and progressive accretionary emplacement. (c) The ophiolite and metamorphic sole obduction and final stage of oceanic closure. AP- accretionary prism, BAB- back-arc basin.

meta-troctolite peak metamorphic conditions (e.g. Peacock, 1988; Wakabayashi and Dilek, 2003). The age of the metamorphism in the Dinaric segment of Tethys is usually placed to the onset of Oxfordian (Lanphere et al., 1975) but a recent study on the Latest Bajocian-Early Bathonian radiolarian assemblages from KKOC suggested a radiolarian deposition to have been contemporaneous to the rapid transitions in the Dinaridic Neotethys geotectonic setting, which changed from active ridge magmatism to an intraoceanic subduction environment and island-arc volcanism (Šegvić et al., 2014). Accordingly, the KKOC metamorphism could have been slightly older than Early Oxfordian. Similar to many Tethyan ophiolites, the KKOC soles were detached from the down-going plate (Fig. 11b) once they have reached its peak metamorphism and were thrust on the Adria margins within the next 10 to 15 Ma (i.e. until the end of Jurassic, Pamić et al., 2002; Bortolotti et al., 2005) (Fig. 11c).

Young subducted mafic rocks were metamorphosed up to granulite, and possibly transitional eclogite-granulite facies, as a consequence of crustal thickening and high temperatures released from the hanging wall of the subduction zone. Taking into account an average geostatic gradient of intraoceanic subduction zones (32 km/GPa) the KKOC soles could have been dragged at maximal depths of ~ 35 km. The thickness of the KKOC is, however, not in favour of such pressures (Roksandić et al., 1971; Pamić et al., 1977). And yet, such discrepancies may be explained by the fact that only part of the upper plate has been obducted on the Adria passive margin but several other interpretations on this topic exist in the literature (e.g. Robertson, 2002). The most widely accepted models assume a thinning of a mantle lithosphere during the prolonged intraoceanic subduction, which in turns leads to extensional disintegration of the overlying ophiolite (Casey and Dewey, 1984; Hacker and Gnos, 1997). The post peak, medium P - high T metamorphic event that gave rise to the equilibrated orthopyroxene blasts in some metagabbros could be related to such pressure release of the system. On the other hand, the high temperatures of metamorphism suggested for analyzed metagabbros and metabasalts must reflect the heat of sub-ophiolite mantle that clearly exceeded 1000 °C (Wakabayashi and Dilek, 2003). This further implies that these rocks were formed proximal to the ridge (Peacock et al., 1994), which fits well with their geochemistry, that turned out to be either of the MORB-like character (with a weak subduction imprint) or have a clear IAT cumulate affiliation. Keeping in mind a geotectonic model proposed above (Fig. 11), the origin of the protoliths of analyzed rocks can be related to the aborted back-arc spreading centre of the upper ophiolite plate (Konjuh). In such a regime, the MORB-like lavas were only marginally affected by subduction fluids, while the IAT lavas were nascent to the gabbro-like cumulates, also suggested by Babajić (2009). Igneous precursors, regardless of their type and exact place of origin in the back-arc realm, were entrained in a subduction zone in the form of olistoliths captured as mélange in the trench (Fig. 11a-b). Further compression resulted in the exhumation of the part of metamorphic sole that suffered different degrees of inverted metamorphism (meta-troctolites vs. metagabbros and metabasalts, Table 6). Exhumed rocks subsequently formed an accretionary wedge that was, thereupon, obducted at the margins of Adria microplate (Pamić et al., 1977) (Fig. 11b-c). Thermal thickening and buoyancy of the fore-back-arc system is actually dependent on its position above the subducted oceanic crust and given the duration of an average subduction cycle of 4 to 5 Ma (time required for subducted material to attain a 120 km depth, Murphy, 2006), the obduction of KKOC must have taken place within the next 10-15 million years as otherwise the upper plate gets too thick and instead of obducting on the continental margin, it bulldozes the margin during the collision. This is well in agreement with the above discussion arguing that the obduction of KKOC ophiolites has been completed by the end of Jurassic (Fig. 11c).

A subduction-accretion-obduction mechanism proposed for the origin of the Krivaja-Konjuh metamorphic sole in the CDOB corresponds to the genetic model argued for the Evia amphibolites from southern and south-eastern Pindos ophiolites (e.g. Robertson, 1991; Gartzos et al., 2009; Fig. 1). It is also very similar to the model proposed by Barth et al. (2008) explaining the origin of the Othris ophiolite in Greece that bears geochemical characteristics of both mid-ocean ridges and supra-subduction zones. According to Jones and Robertson (1991) and Smith and Rassios (2003), intraoceanic subduction processes in this part of Pindos commenced during Middle Jurassic, which coincides with the onset of subduction in CDOB (Lanphere et al., 1975; Šegvić et al., 2014). Such striking similarities in regard to the Tethyan evolution in its Dinaridic and Hellenic branches are strongly in favour of their common tectono-metamorphic history during the Mesozoic era. This corroborates the existence of a single oceanic branch of Neotethys usually referred as Pindos that is nowadays documented by the ophiolites of Bosnia, Serbia, Albania and central Greece (e.g. Stampfli and Borel, 2002; Bortolotti et al., 2005; Gawlick et al., 2008; Barth et al., 2008).

CONCLUSIONS

Metamorphic sole rocks of the Krivaja-Konjuh ophiolite complex from the Central Dinaridic Ophiolite Zone are reported to form an elongated domain between the two main ultramafic masses (Krivaja and Konjuh) having a main metamorphic portion in the southern part of the complex. The rock textures are essentially crystalloblastic to porphyroblastic, whereas analyzed structures are more often than not parallel showing an alternation of ‘white’ and ‘black’ rock domains. Several rock varieties have been recognized forming the KKOC metamorphic sole rocks.

Major and trace element geochemistry and petrographic data showed that most of the KKOC metamorphic sole rocks bear geochemical signatures of mafic gabbroic rocks (SSZ-type setting), whereas the rest corresponds to the more evolved basalts of the tholeiitic affinity (MORB-like-type setting). Geothermobarometric calculations based on the phase chemistry of different coexisting minerals yielded ranges of temperature and pressures for the different KKOC sole varieties. Analyzed soles record a complex metamorphic history that in essence consisted of several steps. The original igneous assemblages were subjected to the high-pressure peak granulite metamorphism at ~ 1.10 to 1.30 GPa and ~ 850 to 1100 °C. The post-peak medium pressure conditions are characterized by decompression and formation of well-preserved coronal reaction textures around garnet and clinopyroxene. It has been further hypothesized that this step is preceded by the pressure-relaxation heating and subsequent growth of orthopyroxene blasts. The last step in the KKOC metamorphic evolution comprises the retrograde greenschist metamorphic overprint, which is marked by the cooling, decompression and hydration.

Metamorphic conditions and field relationships suggest that KKOC soles, derived from mafic gabbroides and tholeiitic basalts, were formed through incipient intraoceanic subduction processes that may have eventually reached deeper lithospheric depths. The generation of the Tethyan oceanic crust in the Dinarides commenced in Late Triassic and continued during the first half of the Jurassic through ocean spreading process. The extensional processes saw an end by the Late Bajocian - Early Bathonian time when an intraoceanic NE subduction took place due to the continuous northwards movement of Africa. The protoliths of analyzed rocks are believed to have been formed in the back-arc setting appearing principally as IAT-type grabbroic rocks or MORB-like-type extrusives. Regardless of protolith type, these mafic rocks must have been affected by intraoceanic subduction process during second half of the Jurassic, which were subsequently exhumed along the ancient subduction channels to form an accretionary wedge that was obducted at the margins of Adria continental microplate. The obduction of the metamorphic sole of the Krivaja-Konjuh ophiolite complex took place in the next 10-15 Ma following the onset of intraoceanic subduction in the Dinaridic part of Neotethys reaching its completion by the end of Jurassic. The proposed formation mechanism and timing of the obduction of the KKOC high-grade metamorphic soles serve an analogue to similar occurrences notably in the central Greek ophiolites which supports the idea of a common tectono-metamorphic history of the Dinaridic-Hellenic branch of Neotethyan during the Mesozoic era.

ACKNOWLEDGEMENTS

Financial support for this work was provided by the German Academic Exchange Service (Stipend to BŠ), Croatian Ministry of Sciences, Education and Sports (195-1951126-3205 to BL), Federal Ministry of Education and Science of Bosnia and Herzegovina (03-39-7194-27/07 to EB), and Research Group of Petrology and Geochemistry at the University of Heidelberg. Hans-Peter Meyer is highly appreciated for providing permanently excellent microprobe facilities. We further extend our acknowledgment to Ilona Finn for providing us with excellent thin sections. The first author is especially in depth to Vesnica Garašić, Vladica Cvetković and Ivan Dragičević for the fruitful scientific discussions. Dejan Prelević, Zoran Jovanović and Gerhard Franz gave valuable comments that helped to improve an early version of the manuscript. Assistance of Goran Rovišan and Zehra Salkić during the fieldwork is greatly appreciated. We thank Aleksandar Ristić and Nabil Shawwa for English improvements. Finally, constructive reviews by Chiara Groppo and Osman Parlak, as well as the editorial handling and suggestions by Alessandra Montanini and Luca Pandolfi, contributed significantly to the manuscript quality.

REFERENCES

Abd El-Naby H., Frisch W. and Hegner E., 2008. Evolution of the Pan-African Wadi Haimur metamorphic sole, Eastern Desert, Egypt. J. Metam. Geol., 18: 639-651. https://doi.org/10.1046/j.1525-1314.2000.00286.x.

Babajić E., 2009. Petrološko-geohemijska obilježja mafitnih stijena Krivajsko-konjuškog ofiolitnog kompleksa. (Dissertation). Univ. Tuzla, Tuzla (in Bosnian with English abstract).

Baldwin J.A., Bowring S.A. and Williams M.L., 2003. Petrological and geochronological constraints on high pressure, high temperature metamorphism in the Snowbird tectonic zone, Canada. J. Metam. Geol., 21: 81-98. https://doi.org/10.1046/j.1525-1314.2003.00413.x.

Barth M.G., Mason P.R.D., Davies G.R. and Drury M.R., 2008. The Othris Ophiolite, Greece: A snapshot of subduction initiation at a mid-ocean ridge. In: Links between ophiolites and LIPs in Earth history. Lithos, 100: 234-254. https://doi.org/10.1016/j.lithos.2007.06.018.

Beccaluva L., Piccardo G.B. and Serri G., 1980. Petrology of Northern Apennine ophiolites and comparision with other Tethyan ophiolites. In: A. Panayiotou (Ed.), Proceed. Intern. Ophiolite Conf., Nicosia, Cyprus, p. 314-331.

Bertrand J., Dietrich V.J., Nievergelt P. and Vaugnat M., 1987. Comparative major and trace element geochemistry of gabbroic and volcanic rock sequences, Montgenèvre ophiolite, Western Alps. Schw. Miner. Petr. Mitt., 67: 147-169.

Bortolotti V., Chiari M., Marroni M., Pandolfi L., Principi G. and Saccani E., 2013. Geodynamic evolution of ophiolites from Albania and Greece (Dinaric-Hellenic belt): one, two, or more oceanic basins? Int. J. Earth Sci., 102: 783-811. https://doi.org/10.1007/s00531-012-0835-7.

Bortolotti V., Marroni M., Pandolfi L. and Principi G., 2005. Mesozoic to Tertiary tectonic history of the Mirdita ophiolites, northern Albania. Isl. Arc, 14: 471-493. https://doi.org/10.1111/j.1440-1738.2005.00479.x.

Boudier F., Bouchez J.L., Nicolas A., Cannat M., Ceuleneer G., Misseri M. and Montigny R., 1985. Kinematics of oceanic thrusting in the Oman ophiolite: model of plate convergence. Earth Planet. Sci. Lett., 75: 215-222. https://doi.org/10.1016/0012-821X(85)90103-7.

Boudier F., Ceuleneer G. and Nicolas A., 1988. Shear zones, thrusts and related magmatism in the Oman ophiolite: Initiation of thrusting on an oceanic ridge. In: F. Boudier and A. Nicolas (Eds.), The ophiolites of Oman. Tectonophysics, 151: 275-296. https://doi.org/10.1016/0040-1951(88)90249-1.

Brandt S., Klemd R. and Okrusch M., 2003. Ultrahigh-temperature metamorphism and multistage evolution of garnet-orthopyroxene granulites from the Proterozoic Epupa Complex, NW Namibia. J. Petrol., 44: 1121-1144. https://doi.org/10.1093/petrology/44.6.1121.

Brey G.P. and Köhler T., 1990. Geothermobarometry in Four-phase Lherzolites II. New thermobarometers, and practical assessment of existing thermobarometers. J. Petrol., 31: 1353-1378. https://doi.org/10.1093/petrology/31.6.1353.

Bucher K. and Frey M., 2002. Petrogenesis of metamorphic rocks, Springer-Verlag, Berlin Heidelberg, 224 pp.

Casey J.F. and Dewey J.F., 1984. Initiation of subduction zones along transform and accreting plate boundaries, triple-junction evolution, and forearc spreading centres. Implications for ophiolitic geology and obduction. Geol. Soc. London Spec. Publ., 13: 269-290. https://doi.org/10.1144/GSL.SP.1984.013.01.22.

Çelik Ö.F. and Delaloye M.F., 2006. Characteristics of ophiolite-related metamorphic rocks in the Beysehir ophiolitic mélange (Central Taurides, Turkey), deduced from whole rock and mineral chemistry. J. Asian Earth Sci., 26: 461-476. https://doi.org/10.1016/j.jseaes.2004.10.008.

Çelik Ö.F., Chiaradia M., Marzoli A., Özkan M., Billor Z. and Topuz G., 2016. Jurassic metabasic rocks in the Kızılırmak accretionary complex (Kargı region, Central Pontides, Northern Turkey). Tectonophysics, 672-673: 34-49. https://doi.org/10.1016/j.tecto.2016.01.043.

Chiari M., Djerić N., Garfagnoli F., Hrvatović H., Krstić M., Levi N., Malasoma A., Marroni M., Menna F., Nirta G., Pandolfi L., Principi G., Saccani E., Stojadinović U. and Trivić B., 2011. The geology of the Zlatibor-Maljen area (Western Serbia): A geotraverse across the ophiolites of the Dinaric-Hellenic collisional belt. Ofioliti, 36: 139-166. https://doi.org/10.4454/ofioliti.V36.I2.3.

Cruciani G., Franceschelli M., Groppo C. and Spano M.E., 2012. Metamorphic evolution of non-equilibrated granulitized eclogite from Punta Li Tulchi (Variscan Sardinia) determined through texturally controlled thermodynamic modelling. J. Metam. Geol., 30: 667-685. https://doi: 10.1111/j.1525-1314.2012.00993.x.

Dangerfield A., Harris R., Sarıfakıoğlu E. and Dilek Y., 2011. Tectonic evolution of the Ankara Mélange and associated Eldivan ophiolite near Hançili, central Turkey. Geol. Soc. Am. Spec. Pap., 480: 143-169. https://doi.org/10.1130/2011.2480(06).

Deer W.A., Howie R.A. and Zussman J., 1996. An introduction to the rock-forming minerals, 2nd Ed., Prentice Hall Ed., Harlow, Essex, England; New York, NY, 498 pp.

D'el-Rey Silva L.J.H., Dantas E.L., Teixeira J.B.G., Laux J.H. and da Silva M.G., 2007. U-Pb and Sm-Nd geochronology of amphibolites from the Curaçá Belt, São Francisco Craton, Brazil: Tectonic implications. Gondw. Res., 12: 454-467. https://doi.org/10.1016/j.gr.2006.11.008.

Dick H.J.B., Natland J.H., Alt J.C., Bach W., Bideau D., Gee J.S., Haggas S., Hertogen J.G.H., Hirth G., Holm P.M., Ildefonse B., Iturrino G.J., John B.E., Kelley D.S., Kikawa E., Kingdon A., LeRoux P.J., Maeda J., Meyer P.S., Miller D.J., Naslund H.R., Niu Y.-L., Robinson P.T., Snow J., Stephen R.A., Trimby P.W., Worm H.-U. and Yoshinobu A., 2000. A long in situ section of the lower ocean crust: results of ODP Leg 176 drilling at the Southwest Indian Ridge. Earth Planet. Sci. Lett., 179: 31-51. https://doi.org/10.1016/S0012-821X(00)00102-3.

Dilek Y. and Flower M.F.J., 2003. Arc-trench rollback and forearc accretion: 2. A model template for ophiolites in Albania, Cyprus, and Oman. Geol. Soc. London Spec. Publ.. 218: 43-68. https://doi.org/10.1144/GSL.SP.2003.218.01.04.

Dimitrijević M.D. and Dimitrijević M.N., 1973. Olistostrome mélange in the Yugoslavian Dinarides and Late Mesozoic plate tectonics. J. Geol., 81: 328-340.

Đorđević D. and Pamić J., 1972. Petrološki izvještaj za osnovnu geološku kartu, list Vlasenica. Federal Geol. Survey, Sarajevo, Belgrade (in Serbian).

Ernst W.G. and Liu J., 1998. Experimental phase-equilibrium study of Al- and Ti-contents of calcic amphibole in MORB; a semiquantitative thermobarometer. Am. Mineral., 83: 952-969. https://doi.org/10.2138/am-1998-9-1004.

Faul U.H., Garapić G. and Lugović B., 2014. Subcontinental rift initiation and ocean-continent transitional setting of the Dinarides and Vardar zone: Evidence from the Krivaja-Konjuh Massif, Bosnia and Herzegovina. Lithos, 202-203: 283-299. https://doi.org/10.1016/j.lithos.2014.05.026.

Ferrière J., Chanier F. and Ditbanjong P., 2012. The Hellenic ophiolites: eastward or westward obduction of the Maliac Ocean, a discussion. Int. J. Earth Sci., 101: 1559-1580. https://doi.org/10.1007/s00531-012-0797-9.

Finger F., Cooke R., Janousek V., Konzett J., Pin C., Roberts M.P. and Tropper P., 2003. Petrogenesis of the south Bohemian granulites: The importance of crystal-melt relationships. J. Geosci., 48: 44-45.

Gaggero L., Marroni M., Pandolfi L. and Buzzi L., 2009. Modeling the oceanic lithosphere obduction: Constraints from the metamorphic sole of Mirdita ophiolites (northern Albania). Ofioliti, 34: 17-42. https://doi.org/10.4454/ofioliti.v34i1.376.

Gartzos E., Dietrich V.J., Migiros G., Serelis K. and Lymperopoulou T., 2009. The origin of amphibolites from metamorphic soles beneath the ultramafic ophiolites in Evia and Lesvos (Greece) and their geotectonic implication. Lithos, 108: 224-242. https://doi.org/10.1016/j.lithos.2008.09.013.

Gawlick H.-J., Frisch W., Hoxha L., Dumitrica P., Krystyn L., Lein R., Missoni S. and Schlagintweit F., 2008. Mirdita Zone ophiolites and associated sediments in Albania reveal Neotethys Ocean origin. Int. J. Earth Sci., 97: 865-881. https://doi.org/10.1007/s00531-007-0193-z.

Gill R., 2010. Igneous rocks and processes: A practical guide, 1st ed., Willey-Blackwell, Oxford, 438 pp.

Gjata K., Kornprobst J., Kodra A., Briot D. and Pineau F., 1992. Subduction chaude a l'aplomb d'une dorsale? Exemple des enclaves de pyroxenite à grenat de la brèche serpentineuse de Derveni (Albanie). Bull. Soc. Géol. Fr., 163: 469-476.

Gnos E. and Kurz D., 1994. Sapphirine-quartz and sapphirine-corundum assemblages in metamorphic rocks associated with the Semail Ophiolite (United Arab Emirates). Contrib. Mineral. Petrol., 116: 398-410. https://doi.org/10.1007/BF00310907.

Gnos E. and Peters T., 1993. K-Ar ages of the metamorphic sole of the Semail Ophiolite: implications for ophiolite cooling history. Contrib. Mineral. Petrol., 113: 325-332. https://doi.org/10.1007/BF00286925.

Godard M., Bosch D. and Einaudi F., 2006. A MORB source for low-Ti magmatism in the Semail ophiolite. Chem. Geol., 234: 58-78. https://doi.org/10.1016/j.chemgeo.2006.04.005.

Gómez-Pugnaire M.T., Azor A., Fernández-Soler J.M. and López Sánchez-Vizcaíno V., 2003. The amphibolites from the Ossa-Morena/Central Iberian Variscan suture (Southwestern Iberian Massif): geochemistry and tectonic interpretation. Lithos, 68: 23-42. https://doi.org/10.1016/S0024-4937(03)00018-5.

Gradstein F.M. and Ogg J.G., 2012. The Chronostratigraphic Scale. In: F.M. Gradstein, J.O. Ogg, M.D. Schmitz and G.M. Ogg (Eds.), The Geologic Time Scale. Elsevier, Boston, pp. 31-42.

Graham C.M. and Powell R., 1984. A garnet-hornblende geothermometer: calibration, testing, and application to the Pelona Schist, Southern California. J. Metam. Geol., 2: 13-31. https://oi.org/10.1111/j.1525-1314.1984.tb00282.x.

Groppo C., Rolfo F., Liu Y.-C. Deng, L.-P. and Wang A.-D., 2015. P-T evolution of elusive UHP eclogites from the Luotian dome (North Dabie Zone, China): How far can the thermodynamic modeling lead us? Lithos, 226: 183-200. https://doi: 10.1016/j.lithos.2014.11.013.

Guilmette C., Hébert R., Dupuis C., Wang C. and Li Z., 2008. Metamorphic history and geodynamic significance of high-grade metabasites from the ophiolitic mélange beneath the Yarlung Zangbo ophiolites, Xigaze area, Tibet. The origin and tectonic setting of ophiolites in China. J. Asian Earth Sci., 32: 423-437. https://doi.org/10.1016/j.jseaes.2007.11.013.

Guilmette C., Hébert R., Wang C. and Villeneuve M., 2009. Geochemistry and geochronology of the metamorphic sole underlying the Xigaze Ophiolite, Yarlung Zangbo Suture Zone, South Tibet. In: Y. Niu (Ed.), Recent developments on seafloor petrology and tectonics. A volume in honour of Roger Hekinian for his life-long contributions to marine petrology and tectonics research. Lithos, 112: 149-162. https://doi.org/10.1016/j.lithos.2009.05.027.

Hacker B.R., 1990. Simulation of the metamorphic and deformational history of the metamorphic sole of the Oman Ophiolite. J. Geoph. Res. Solid Earth, 95: 4895-4907. https://doi.org/10.1029/JB095iB04p04895.

Hacker B.R., 1991. The role of deformation in the formation of metamorphic gradients: Ridge subduction beneath the Oman Ophiolite. Tectonics, 10: 455-473. https://doi.org/10.1029/90TC02779.

Hacker B.R. and Gnos E., 1997. The conundrum of Samail: explaining the metamorphic history. In: D. Mainprice, F. Boudier and J.-L. Bouchez (Eds.), The Adolphe Nicolas Volume. Tectonophysics 279: 215-226. https://doi.org/10.1016/S0040-1951(97)00114-5.

Hacker B.R. and Mosenfelder J.L., 1996. Metamorphism and deformation along the emplacement thrust of the Samail ophiolite, Oman. Earth Planet. Sci. Lett., 144: 435-451. https://doi.org/10.1016/S0012-821X(96)00186-0.

Harley S.L., 1984. An experimental study of the partitioning of Fe and Mg between garnet and orthopyroxene. Contrib. Mineral. Petrol., 86: 359-373. https://doi.org/10.1007/BF01187140.

Harley S.L., 1989. The origins of granulites: a metamorphic perspective. Geol. Mag., 126: 215-247. https://doi: 10.1017/S0016756800022330.

Harley S.L. and Green D.H., 1982. Garnet-orthopyroxene barometry for granulites and peridotites. Nature, 300: 697-701. https://doi.org/10.1038/300697a0.

Harlov D., Tropper P., Seifert W., Nijland T. and Förster H.-J., 2006. Formation of Al-rich titanite ($CaTiSiO_4O$-$CaAlSiO_4OH$) reaction rims on ilmenite in metamorphic rocks as a function of fH_2O and fO_2. In: J.M. Pyle and J.A. Baldwin (Eds.), Compositional variation in metamorphic accessory phases AGU-CGU Joint Assembly. Lithos, 88: 72-84. https://doi.org/10.1016/j.lithos.2005.08.005.

Harper G.D., Grady K. and Coulton A.J., 1996. Origin of the amphibolite "sole" of the Josephine ophiolite: Emplacement of a cold ophiolite over a hot arc. Tectonics 15: 296-313. https://doi: 10.1029/95TC02525.

Hart S.R., Blusztajn J., Dick H.J.B., Meyer P.S. and Muehlenbachs K., 1999. The fingerprint of seawater circulation in a 500-meter section of ocean crust gabbros. Geochim. Cosmochim. Acta, 63: 4059-4080. https://doi.org/10.1016/S0016-7037(99)00309-9.

Higgins J.B. and Ribbe P.H., 1976. The crystal chemistry and space groups of natural and synthetic titanites. Am. Mineral., 61: 878-888.

Holland T. and Blundy J., 1994. Non-ideal interactions in calcic amphiboles and their bearing on amphibole-plagioclase thermometry. Contrib. Mineral. Petrol., 116: 433-447. https://doi.org/10.1007/BF00310910.

Hrvatović H., 2006. Geološki vodić kroz Bosnu i Hercegovinu, Geological Survey of Federation of Bosnia and Herzegovina, Sarajevo (Ilidža), 203 pp. (in Bosnian with English abstract).

Hwang S.L., Yui T.F., Chu H.T., Shen P., Schertl H.P., Zhang R.Y. and Liou J.G., 2007. On the origin of oriented rutile needles in garnet from UHP eclogites. J. Metam. Geol., 25: 349-362. https://doi.org/10.1111/j.1525-1314.2007.00699.x.

Ikeda Y., 1990. CeN/ SrN/ SmN; a trace element discriminant for basaltic rocks from different tectonomagmatic environments. N. Jb. Mineral., Hefte 4: 145-159.

Ikeda Y., Kimura M., Mori H. and Takeda H., 1981. Chemical composition of matrices of unequilibrated ordinary chondrites. In: 6th Symp. on Antarctic Meteorites. Nat. Inst. Polar Res., Tokyo, p. 124-144.

Ilnicki S., 2002. Amphibolites and metabasites from the Izera block, West Sudetes. Mineral. Soc. Pol. Spec. Pap., 20: 262-269.

Jamieson R.A., 1986. P-T paths from high temperature shear zones beneath ophiolites. J. Metam. Geol., 4: 3-22. https://doi.org/10.1111/j.1525-1314.1986.tb00335.x.

Jaques A.L., Chappell B.W. and Taylor S.R., 1983. Geochemistry of cumulus peridotites and gabbros from the Marum ophiolite complex, northern Papua New Guinea. Contrib. Mineral. Petrol., 82: 154-164. https://doi.org/10.1007/BF01166610.

Jones G. and Robertson A.H.F., 1991. Tectono-stratigraphy and evolution of the Mesozoic Pindos ophiolite and related units, northwestern Greece. J. Geol. Soc. London, 148: 267-288. https://doi.org/10.1144/gsjgs.148.2.0267.

Jovanović R., 1961. Prilog poznavanju prostranstva i facija mezozoika "Unutrašnje zone Dinarida" u NR BiH, IIIème Congrès des geologues de Yugoslavie, L'union des sociétés géologiques de la RFP de Yugoslavie, Budva, p. 148-176 (in Serbian with English abstract).

Karamata S., 2006. The geological development of the Balkan Peninsula related to the approach, collision and compression of Gondwanan and Eurasian units. Geol. Soc. London Spec. Publ., 260: 155-178. https://doi.org/10.1144/GSL.SP.2006.260.01.07.

Karamata S., Sladić-Trifunović M., Cvetković V., Milovanović D., Resimić-Šarić K., Olujić J., and Vujnović L., 2005. The western belt of the Vardar zone with special emphasis to the ophiolites rocks of the Balkan Peninsula. Bull. Acad. Serbe Sci. Arts Cl. Sci. Mathém. Nat., Sci. Nat., 43: 85-96.

Kretz R., 1983. Symbols for rock-forming minerals. Am. Mineral., 68: 277-279.

Krogh E.J., 1988. The garnet-clinopyroxene Fe-Mg geothermometer - A reinterpretation of existing experimental data. Contrib. Mineral. Petrol., 99: 44-48. https://doi.org/10.1007/BF00399364.

Krogh Ravna E., 2000. Distribution of Fe^{2+} and Mg between coexisting garnet and hornblende in synthetic and natural systems: an empirical calibration of the garnet-hornblende Fe-Mg geothermometer. Lithos, 53: 265-277. https://doi.org/10.1016/S0024-4937(00)00029-3.

Langmuir C.H., Klein E.M. and Plank T., 1992. Petrological Systematics of mid-ocean ridge basalts: Constraints on melt generation beneath ocean ridges. In: J.P. Morgan, D.K. Blackman and J.M. Sinton (Eds.), Mantle flow and melt generation at mid-ocean ridges. Am. Geophys. Union, p. 183-280. https://doi.org/10.1029/GM071p0183.

Lanphere M.A., Coleman R.G., Karamata S. and Pamić J., 1975. Age of amphibolites associated with Alpine peridotites in the Dinaride ophiolite zone, Yugoslavia. Earth Planet. Sci. Lett., 26: 271-276. https://doi.org/10.1016/0012-821X(75)90001-1.

Lázaro C., Blanco-Quintero I.F., Rojas-Agramonte Y., Proenza J.A., Núñez-Cambra K. and García-Casco A., 2013. First description of a metamorphic sole related to ophiolite obduction in the northern Caribbean: Geochemistry and petrology of the Güira de Jauco Amphibolite complex (eastern Cuba) and tectonic implications. Lithos, 179: 193-210. https://doi.org/10.1016/j.lithos.2013.08.019.

Leake B.E., Woolley A.R., Arps C.E.S., Birch W.D., Gilbert M.C., Grice J.D., Hawthorne F.C., Kato A., Kisch H.J., Krivovichev V.G., Linthout K., Laird J., Mandarino J.A., Maresch W.V., Nickel E.H., Rock N.M.S., Schumacher J.C., Smith D.C., Stephenson N.C.N., Ungaretti L., Whittaker E.J.W. and Youzhi G., 1997. Nomenclature of amphiboles; Report of the Subcomm. on Amphiboles Intern. Miner. Ass., Commiss. New Minerals and Mineral Names. Am. Mineral., 82: 1019-1037.

Lee H.Y. and Ganguly J., 1988. Equilibrium compositions of coexisting garnet and orthopyroxene: experimental determinations in the System FeO-MgO-Al^2O^3-SiO^2, and applications. J. Petrol., 29: 93-113. https://doi.org/10.1093/petrology/29.1.93.

Liati A., 1988. Amphibolitized eclogites in the Rhodope-Crystalline Complex, near Xanthi (N. Greece). N. Jb. Mineral. Monatsh., 1: 1-8.

Lugović B., Altherr R., Raczek I., Hofmann A.W. and Majer V., 1991. Geochemistry of peridotites and mafic igneous rocks from the Central Dinaric Ophiolite Belt, Yugoslavia. Contrib. Mineral. Petrol., 106: 201-216. https://doi.org/10.1007/BF00306434.

Majer V. and Lugović B., 1985. Metamorphic rocks from the Ophiolite zone in Banija, Yugoslavia: amphibolites. Acta Geol. Zagreb, 15: 1-25.

Maksimović Z. and Majer V., 1981. Accessory spinels of two main zones of Alpine ultramafic rocks in Yugoslavia. Bull. Acad. Serbe Sci. Arts, 21: 13-26.

Maksimović Z. and Kolomejceva-Jovanović L., 1987. Sastav koegzistirajucih minerala peridotita Jugoslavije i problemi geotermometrije i geobarometrije ultramafitskih zona. Bull. Acad. Serbe Sci. Arts, 345, 21-52 (in Serbian with English abstract).

McDonough W.F. and Sun S.-S., 1995. The composition of the Earth. In: Chemical evolution of the mantle. Chem. Geol., 120: 223-253. https://doi.org/10.1016/0009-2541(94)00140-4.

Meinhold G., Anders B., Kostopoulos D. and Reischmann T., 2008. Rutile chemistry and thermometry as provenance indicator: An example from Chios Island, Greece. Sedim. Geol., 203: 98-111, doi: 10.1016/j.sedgeo.2007.11.004.

Milovanović D., Tucci P., Morbidelli P. and Popović D., 2004. Petrology of mafic granulites from Bistrica, southern part of Zlatibor ultramafic massif (Dinaridic Ophiolites belt, Serbia). In: 32th Intern. Geol. Congr., Florence, Italy. Abstr. Book, p. 21-23.

Moazzen M. and Oberhänsli R. 2008. Whole rock and relict igneous clinopyroxene geochemistry of ophiolite-related amphibolites from NW Iran. Implications for protolith nature. N. Jb. Mineral., Abh., 185: 51-62. https://doi: 10.1127/0077-7757/2008/0106.

Morimoto N., 1988. Nomenclature of pyroxenes. Mineral. Petrol., 39: 55-76. https://doi: 10.1007/BF01226262.

Mukhopadhyay B. and Bose M.K., 1994. Transitional granulite-eclogite facies metamorphism of basic supracrustal rocks in a shear zone complex in the Precambrian shield of South India. Mineral. Mag., 58: 97-118.

Murphy J.B., 2006. Igneous rock associations 7. Arc magmatism I: Relationship between subduction and magma genesis. Geosci. Can., 33: 145-167.

Newton R.C. and Perkins D., 1982. Thermodynamic calibration of geobarometers based on the assemblages garnet-plagioclase-orthopyroxene (clinopyroxene)-quartz. Am. Mineral., 67: 203-222.

Nickel K.G. and Green D.H., 1985. Empirical geothermobarometry for garnet peridotites and implications for the nature of the lithosphere, kimberlites and diamonds. Earth Planet. Sci. Lett., 73: 158-170. https://doi.org/10.1016/0012-821X(85)90043-3.

Okrusch M., Seidel E., Kreuzer H. and Harre W., 1978. Jurassic age of metamorphism at the base of the Brezovica peridotite (Yugoslavia). Earth Planet. Sci. Lett., 39: 291-297. https://doi.org/10.1016/0012-821X(78)90205-4.

Operta M., Pamić J., Balen D. and Tropper P., 2003. Corundum-bearing amphibolites from the metamorphic basement of the Krivaja-Konjuh ultramafic massif (Dinaride Ophiolite Zone, Bosnia). Mineral. Petrol., 77: 287-295. https://doi.org/10.1007/s007100300002.

Palinkaš A.L., Borojević Šoštarić S., Neubauer F. and Cvetković V., 2008. Amphibolite sole in the Rogozna Mt., Western Vardar ophiolite belt, N. Kosovo. In: F. Neubauer (Ed.), Ophiolites and the palaeogeographic and tectonic reconstruction of the Alpine-Carpathian-Dinaric Orogenic Belt. Univ. Salzburg, Salzburg, p. 26.

Pamić J., 1968. Petrološki izvještaj za tumač lista Zavidovići, Scale 1:100000 osnovne geološke karte SFRJ. Geol. Survey - Federal Geological Survey, Sarajevo, Belgrade (in Croatian with English abstract).

Pamić J., 1970. Petrološki izvještaj za tumač lista Vareš, Scale 1:100000 osnovne geološke karte SFRJ. Geol. Survey - Federal Geol. Survey, Sarajevo, Belgrade.

Pamić J. and Desmons J., 1989. A complete ophiolite sequence in Rzav, area of Zlatibor and Varda ultramafic massifs, the Dinaride Ophiolite Zone. Ofioliti, 14: 13-32.

Pamić J. and Hrvatović H., 2000. Dinaride Ophiolite Zone (DOZ). Basic data on the geology and petrology of the Krivaja-Konjuh ophiolite complex. Pancardi 2000 Fieldtrip Guidebook. Vijesti Hrvat. Geol. Druš., 37: 60-68.

Pamić J. and Majer V., 1973. Eclogites and amphibolites from Crni Potok on the southern border of the Borja ultramafic massif in Bosnia (Yugoslavia). Geol. Glasn., 17: 119-131.

Pamić J., Gušić I. and Jelaska V., 1998. Geodynamic evolution of the Central Dinarides. Tectonophysics, 297: 251-268. https://doi.org/10.1016/S0040-1951(98)00171-1.

Pamić J., Šćavničar S. and Medjimorec S., 1973. Mineral assemblages of amphibolites associated with Alpine-type ultramafics in the Dinaride Ophiolite Zone (Yugoslavia). J. Petrol., 14: 133-157. https://doi.org/10.1093/petrology/14.1.133.

Pamić J., Tomljenović B. and Balen D., 2002. Geodynamic and petrogenetic evolution of Alpine ophiolites from the central and NW Dinarides: an overview. In: V. Hoeck, A.H.F. Robertson, F. Koller and C. Tomek (Eds.), Eastern Mediterranean Ophiolites: Magmatic processes and geodynamic implications, held at the 10th Meeting of the Eur. Union Geosci., Strasbourg, France, March-April, 1999. Lithos, 65: 113-142. https://doi.org/10.1016/S0024-4937(02)00162-7.

Paria P., Bhattacharya A. and Sen S.K., 1988. The reaction garnet + clinopyroxene + quartz = 2 orthopyroxene + anorthite: A potential geobarometer for granulites. Contrib. Mineral. Petrol., 99: 126-133. https://doi.org/10.1007/BF00399372.

Peacock S.M., 1988. Inverted metamorphic gradients in the westernmost Cordillera. In: W.G. Ernst (Ed.), Metamorphism and crustal evolution of the Western U. S. New Jersey. Rubey Vol. 7: 954-975.

Peacock S.M., Rushmer T. and Thompson A.B., 1994. Partial melting of subducting oceanic crust. Earth Planet. Sci. Lett., 121: 227-244. https://doi.org/10.1016/0012-821X(94)90042-6.

Pearce J.A. and Norry M.J., 1979. Petrogenetic implications of Ti, Zr, Y, and Nb variations in volcanic rocks. Contrib. Mineral. Petrol., 69: 33-47. https://doi.org/10.1007/BF00375192.

Perkins D. and Chipera S.J., 1985. Garnet-orthopyroxene-plagioclase-quartz barometry: refinement and application to the English River subprovince and the Minnesota River valley. Contrib. Mineral. Petrol., 89: 69-80. https://doi.org/10.1007/BF01177592.

Plyusnina L.P., 1982. Geothermometry and geobarometry of plagioclase-hornblende bearing assemblages. Contrib. Mineral. Petrol., 80: 140-146. https://doi.org/10.1007/BF00374891.

Popević A. and Pamić J., 1973. Corundum amphibolite schists from the Bistrica amphibolites, southern margin of the Zlatibor massif. Glasn. Prir. Muzeja Srp. Zemlje, p. 31-39.

Pouchou J.L. and Pichoir F., 1984. A new model for quantitative analyses. I. Application to the analysis of homogeneous samples. Rech. Aérospat., 3: 1-38.

Pouchou J.L. and Pichoir F., 1985. "PAP" (ϕ-ϱ-Z) correction procedure for improved quantitative microanalysis. In: J.T. Armstrong (Ed.), Microbeam analysis. San Francisco, p. 104-106.

Raase P., Raith M., Ackermand D. and Lal R.K., 1986. Progressive metamorphism of mafic rocks from greenschist to granulite facies in the Dharwar Craton of South India. J. Geol., 94: 261-282.

Rasool Q., Ramanujam N. and Biswas S.K., 2015. Petrology and geochemistry of gabbros from the Andaman Ophiolite: Implications for their petrogenesis and tectonic setting. J. Geol. Geophys., 4: 226. https://doi.org/10.4172/2381-8719.1000226.

Reagan M.K. and Meijer A., 1984. Geology and geochemistry of early arc-volcanic rocks from Guam. Geol. Soc. Am. Bull., 95: 701-713. https://doi.org/10.1130/0016-7606(1984)95<701:GAGOEA>2.0.CO;2.

Ristić P. and Likar J., 1967. Magmatizam i geohemizam planine Konjuh. Ibid 3-4: 3-17 (in Serbian with English abstract).

Robertson A.H.F., 1991. Origin and emplacement of an inferred late Jurassic subduction-accretion complex, Euboea, eastern Greece. Geol. Mag., 128: 27-41. https://doi.org/10.1017/S0016756800018021.

Robertson A.H.F., 2002. Overview of the genesis and emplacement of Mesozoic ophiolites in the Eastern Mediterranean Tethyan region. In: V. Hoeck, A.H.F. Robertson, F. Koller and C. Tomek (Eds.), Eastern Mediterranean Ophiolites: Magmatic processes and geodynamic implications, held at the 10th Meeting of the Eur. Union Geosci., Strasbourg, France, March-April, 1999. Lithos, 65: 1-67. https://doi.org/10.1016/S0024-4937(02)00160-3.

Robertson A.H.F. and Karamata S., 1994. The role of subduction-accretion processes in the tectonic evolution of the Mesozoic Tethys in Serbia. In: Y. Mart and J. Woodside (Eds.), Tectonic processes of the Eastern Mediterranean and analogous region. Tectonophysics, 234: 73-94. https://doi.org/10.1016/0040-1951(94)90205-4.

Robertson A.H.F., Trivić B., Đerić N. and Bucur I.I., 2013. Tectonic development of the Vardar ocean and its margins: Evidence from the Republic of Macedonia and Greek Macedonia. In: D. Papanikolaou, G Roberts and L. Royden (Eds.), The Agean: A natural laboratory for tectonics-tectonometamorphics. Tectonophysics, 595-596: 25-54. https://doi.org/10.1016/j.tecto.2012.07.022.

Roksandić M.M., 1971. Geotektonski položaj i oblik velikih peridotitskih masiva Dinarida u svetlosti geofizičkih podataka. Vesti Zavoda Za Geol. Istraživanja Beograd, p. 139-147 (in Serbian with English abstract).

Romano S.S., Brix M.R., Dörr W., Fiala J., Krenn E. and Zulauf G., 2006. The Carboniferous to Jurassic evolution of the pre-Alpine basement of Crete: constraints from U-Pb and U-(Th)-Pb dating of orthogneiss, fission-track dating of zircon, structural and petrological data. J. Geol. Soc. London Spec. Publ., 260: 69-90. doi: 10.1144/GSL.SP.2006.260.01.05.

Rutland R.W.R. and Sutherland D., 1968. The chemical composition of granitic gneisses and spargamitic meta-sediments in the Glomfjord region, Northern Norway. Nor. Geol. Tidsskr., 48: 365-380.

Saccani E., Beccaluva L., Photiades A. and Zeda O., 2011. Petrogenesis and tectono-magmatic significance of basalts and mantle peridotites from the Albanian-Greek ophiolites and sub-ophiolitic mélanges. New constraints for the Triassic-Jurassic evolution of the Neo-Tethys in the Dinaride sector. In: A. Montanini, G.B. Piccardo, R. Tribuzio and H.J.B. Dick (Eds.)., Alpine ophiolites and modern analogues: Continental rifting to oceanic lithosphere. Lithos, 124: 227-242. https://doi.org/10.1016/j.lithos.2010.10.009.

Saunders A.D., 1984. The Rare Earth element characteristics of igneous rocks from the ocean basins, Chapter 6. In: P. Henderson (Ed.), Developments in geochemistry, Rare Earth element geochemistry. Elsevier, p. 205-236.

Schmid S.M., Bernoulli D., Fügenschuh B., Matenco L., Schefer S., Schuster R., Tischler M. and Ustaszewski K., 2008. The Alpine-Carpathian-Dinaridic orogenic system: correlation and evolution of tectonic units. Swiss J. Geosci., 101: 139-183. https://doi.org/10.1007/s00015-008-1247-3.

Schmidt M.W., 1992. Amphibole composition in tonalite as a function of pressure: an experimental calibration of the Al-in-hornblende barometer. Contrib. Mineral. Petrol., 110: 304-310. https://doi.org/10.1007/BF00310745.

Šegvić B., 2010. Petrologic and geochemical characteristics of the Krivaja-Konjuh ophiolite complex (NE Bosnia and Herzegovina) - Petrogenesis and regional geodynamic implications (PhD Thesis). Ruprecht-Karls-Univ. Heidelberg, Heidelberg, 193 pp.

Šegvić B., Kukoč D., Dragičević I., Vranjković A., Brčić V., Goričan Š., Babajić E. and Hrvatović H., 2014. New record of Middle Jurassic radiolarians and evidence of Neotethyan dynamics documented in a mélange from the Central Dinaridic Ophiolite Belt (CDOB, NE Bosnia and Herzegovina). Ofioliti, 39 (1): 33-43. https://doi.org/10.4454/ofioliti.v39i1.427.

Šegvić B., Lugović B., Slovenec D. and Meyer H.-P., 2016. Mineralogy, petrology and geochemistry of amphibolites from the Kalnik Mt. (Sava Unit, North Croatia): Implications for the evolution of north-westernmost part of the Dinaric-Vardar branch of Mesozoic Tethys. Ofioliti, 41: 35-58. https://doi.org/10.4454/ofioliti.v41i1.441

Sen S.K. and Oliver R.L., 1981. Secondary hornblendes in some granulite fades rocks from the Mann Ranges, Australia. J. Geol. Soc. Austr., 28: 137-140. https://doi.org/10.1080/00167618108729152.

Serri G. and Saitta M., 1980. Fractionation trends of the gabbroic complexes from high-Ti and low-Ti ophiolites and the crust of major oceanic basins: a comparison. Ofioliti, 5: 241-264.

Shervais J.W., 1982. Ti-V plots and the petrogenesis of modern and ophiolitic lavas. Earth Planet. Sci. Lett., 59: 101-118. https://doi.org/10.1016/0012-821X(82)90120-0.

Smith A.G. and Rassios A., 2003. The evolution of ideas for the origin and emplacement of the western Hellenic ophiolites. Geol. Soc. Am. Spec. Pap., 37: 337-350. https://doi.org/10.1130/0-8137-2373-6.33.

Smith A.G. and Spray J.G., 1984. A half-ridge transform model for the Hellenic-Dinaric ophiolites. In: J.E. Dixon and A.H.F. Robertson (Eds.), Geol. Soc. London Spec. Publ., 17: 629-644.

Spear F.S., 1980. NaSi CaAl exchange equilibrium between plagioclase and amphibole. Contrib. Mineral. Petrol., 7: 33-41. https://doi.org/10.1007/BF00375566.

Spray J.G., 1984. Possible causes and consequences of upper mantle decoupling and ophiolite displacement. Geol. Soc. London Spec. Publ., 13: 255-268. https://doi.org/10.1144/GSL.SP.1984.013.01.21.

Srećković-Batoćanin D., Milovanović D. and Balogh K., 2002. Petrology of the garnet amphibolites from the Tejići Village - Povlen Mt., Western Serbia. Geol. Anali Balk., Poluostrva, 64: 187-198.

Stampfli G.M. and Borel G.D., 2002. A plate tectonic model for the Paleozoic and Mesozoic constrained by dynamic plate boundaries and restored synthetic oceanic isochrons. Earth Planet. Sci. Lett., 196: 17-33. https://doi.org/10.1016/S0012-821X(01)00588-X.

Šuica S., Lugović B. and Kukoč D., 2018. Tectono-magmatic significance of the pillow basalts from the ophiolitic mélange of the Dinarides. Ofioliti, 43: 85-101. https://doi.org/10.4454/ofioliti.v43i1.506.

Sun S. and McDonough W.F., 1989. Chemical and isotopic systematics of oceanic basalts: implications for mantle composition and processes. Geol. Soc. London Spec. Publ., 42: 313-345. https://doi.org/10.1144/GSL.SP.1989.042.01.19.

Tari V., 2002. Evolution of the northern and western Dinarides: a tectonostratigraphic approach. In: G. Bertotti, K. Schulmann and S. Cloetingh (Eds.), Continental collision and the tectonosedimentary evolution of forelands. EGU Stephan Mueller Spec. Publ. Series, 1 (1-2): 223-236.

Thy P., 2003. Igneous petrology of gabbros from Hole 1105A: Oceanic magma chamber processes. In: J.F. Casey and D.J. Miller (Eds.), Proceed. ODP, Sci. Results, p. 1-76.

Tremblay A., Meshi A., Deschamps T., Goulet F. and Goulet N., 2015. The Vardar zone as a suture for the Mirdita ophiolites, Albania: Constraints from the structural analysis of the Korabi-Pelagonia zone. Tectonics. 34: 352-375. https://doi.org/10.1002/2014TC003807.

Trubelja F., 1961. Magmatske stijene jugoistočnog dijela planine Konjuh (Bosna). Geol. Glasnik, 5, 241-262 (in Croatian with English abstract).

Trubelja F., Marchig V., Burgath K.P. and Vujović Ž., 1995. Origin of the Jurassic Tethyan ophiolites in Bosnia: A geochemical approach to tectonic setting. Geol. Croat., 48: 49-66.

Ustaszewski K., Kounov A., Schmid S.M., Schaltegger U., Krenn E., Frank W. and Fügenschuh B., 2010. Evolution of the Adria-Europe plate boundary in the northern Dinarides: From continent-continent collision to back-arc extension. Tectonics, 29: TC6017. https://doi.org/10.1029/2010TC002668.

Vishnevskaya V.S., Djeric N. and Zakariadze G.S., 2009. New data on Mesozoic Radiolaria of Serbia and Bosnia, and implications for the age and evolution of oceanic volcanic rocks in the Central and Northern Balkans. In: A.H.F. Robertson, S. Karamata and K. Šarić (Eds.), Ophiolites and related geology of the Balkan region. Lithos, 108: 72-105. https://doi.org/10.1016/j.lithos.2008.10.015.

Wakabayashi J. 2004., Tectonic mechanisms associated with P-T paths of regional metamorphism: alternatives to single-cycle thrusting and heating. Tectonophysics, 392: 193-218.

Wakabayashi J. and Dilek Y., 2000. Spatial and temporal relationships between ophiolites and their metamorphic soles: A test of models of forearc ophiolite genesis. In: Y. Dilek, E.M. Moores, D. Elthon and A. Nicolas (Eds.), Ophiolites and oceanic crust: New insights from field studies and the Ocean Drilling Program. Geol. Soc. Am. Spec. Pap., 349: 53-64. https://doi.org/10.1130/0-8137-2349-3.53.

Wakabayashi J. and Dilek Y., 2003. What constitutes 'emplacement' of an ophiolite?: Mechanisms and relationship to subduction initiation and formation of metamorphic soles. Geol. Soc. London Spec. Publ., 218: 427-447. https://doi.org/10.1144/GSL.SP.2003.218.01.22.

Wankang H., Junwen W., Basu A.R. and Tatsumoto M., 1993. A study of REE and Pb, Sr and Nd isotopes in garnet-lherzolite xenoliths from Mingxi, Fujian Province. Chin. J. Geochem., 12: 97-109. https://doi.org/10.1007/BF02842191.

Wells P.R.A., 1977. Pyroxene thermometry in simple and complex systems. Contrib. Mineral. Petrol., 62: 129-139. https://doi.org/10.1007/BF00372872.

Williams R., 1984. Field relations and chemistry of sapphirine bearing rocks from the Rørnesund area. Fiskenesset, Western Greenland. Can. Mineral., 22: 417-421.

Woodsworth G.J., 1977. Homogenization of zoned garnets from pelitic schists. Can. Mineral., 15: 230-242.

Wolf M.B. and Wyllie P.J., 1993. Garnet growth during amphibolite anatexis: Implications of a garnetiferous restite. J. Geol., 101: 357-373.

Wood D.A., 1980. The application of a Th-Hf-Ta diagram to problems of tectonomagmatic classification and to establishing the nature of crustal contamination of basaltic lavas of the British Tertiary Volcanic Province. Earth Planet. Sci. Lett., 50: 11-30. https://doi.org/10.1016/0012-821X(80)90116-8.

Wood B.J. and Banno S., 1973. Garnet-orthopyroxene and orthopyroxene-clinopyroxene relationships in simple and complex systems. Contrib. Mineral. Petrol., 42: 109-124. https://doi.org/10.1007/BF00371501.

Received, March 27, 2018
Accepted, September 7, 2018